DOI: 10.1111/mice.12783

ORIGINAL ARTICLE

COMPUTER-AIDED CIVIL AND INFRASTRUCTURE ENGINEERING WILEY

A deterministic algorithm for nonlinear, fatigue-based structural health monitoring

Dimitrios Pavlou

Department of Mechanical and Structural Engineering and Materials Science, University of Stavanger,Stavanger, Norway

Correspondence
Dimitrios Pavlou, Department of Mechanical and Structural Engineering and Materials Science, University of Stavanger, Norway.
Email: dimitrios.g.pavlou@uis.no

Abstract

The irregularity of peak and valley stress values of loading histories is the main impediment for accurate fatigue-based structural health monitoring. Since the available fatigue material data (e.g., S-N curves) have been derived by cyclic loading tests, and the existing damage accumulation models can be implemented on structures under cyclic loading, cycle-counting algorithms for the transformation of a spectrum loading into an equivalent cyclic one are necessary for deterministic fatigue damage estimation and life prediction. The existing four cycle-counting algorithms have an inherent disadvantage; the sequence of the derived cycles is unknown, and the loading sequence effect on the fatigue damage estimation and life prediction cannot be accounted for (linear damage summation). The present work proposes a new damage estimation algorithm containing two modules: a new cycle-counting algorithm and a new damage summation algorithm. Unlike the existing methods, the proposed algorithm takes into account the loading sequence effect and has a solid physical base because it simulates the nonlinear damage accumulation with a multi-linear damage summation procedure. With the aid of a new concept of inserting fictitious loading cycles in the irregular spectrum, the proposed cycle counting module counts loading cycles that correspond to loading loops with an algorithm that is easily applicable in engineering practice. According to the author's knowledge, nonlinear damage accumulation estimation in structures under an irregular loading spectrum is carried out for the first time. The effect of the loading sequence to high-low two-stage random loading, low-high two-stage random loading, decreasing amplitude multi-stage random loading, increasing amplitude multi-stage random loading, and alternating amplitude random loading is examined and discussed.

1 | INTRODUCTION

A service loading of infrastructures subjected to environmental loads consists of irregular stress histories. The loading spectra contain reversals instead of loading cycles (Figure 1). Existing methods for structural health monitoring and structural integrity of structures subjected to spectrum loading are classified into two categories: (a) machine

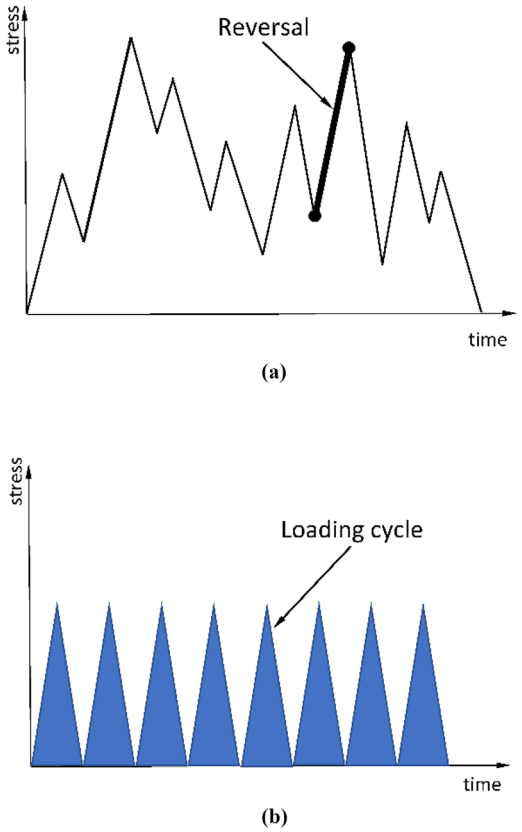

FIGURE 1 (a) "Irregular" loading history, that is, loading history containing reversals, (b) "cyclic" loading history, that is, loading history containing full cycles

learning (ML) algorithms, and (b) fatigue damage-based methods.

1.1 | ML algorithms in structural integrity and health monitoring

Application of artificial intelligence (AI) in civil/structural engineering was pioneered by Adeli and colleagues in the mid-1980s, in a field known to be skeptical and averse to new technologies (Adeli & Al-Rijleh, 1987; Adeli & Balasubramanyam, 1988a, 1988b; Adeli & Paek, 1986a, 1986b; Paek & Adeli, 1988, 1988b). Those early research articles were followed by a seminal book titled *Expert Systems for Structural Design—A New Generation* (Adeli & Balasubramanyam, 1988).

The first journal article on civil/structural engineering applications of neural networks was published by Adeli and Yeh (1989). A year later, Adeli and Yeh (1990) presented an explanation-based ML in engineering design. Hojjat Adeli is known as one of the founders of knowledge engineering as established by the noted biographer Weingardt (2010). These early highly influential and trailblazing works have had a profound impact on the application of AI in civil/structural engineering over the past 35 years, which is why Hojjat Adeli is widely recognized as the father of AI and ML in civil engineering.

In the early 1990s, Adeli pioneered the fields of computational intelligence (CI) through a multiparadigm approach and adroit integration of three separate CI or soft computing paradigms, that is, neural networks, genetic algorithms, and fuzzy logic (Adeli & Hung, 1994; Hung & Adeli, 1993, 1994). His book *Machine Learning–Neural Networks, Genetic Algorithms, and Fuzzy Systems* (Adeli & Hung, 1995) was the first authored book that presented and integrated the three main fields of CI in a single volume and demonstrated how a multi-paradigm approach could solve the ML problems more effectively. Later, Ahmadlou and Adeli (2010) developed a robust classifier, the enhanced probabilistic neural network with local decision circles.

More recently, Rafiei and Adeli (2017a) developed a new and powerful neural dynamic classification algorithm that has been used successfully to solve complicated classification problems such as damage detection in high-rise building structures (Rafiei & Adeli, 2017b) and earthquake prediction (Rafiei & Adeli, 2017c). Deep neural network learning has been the subject of intense research in recent years (Lara-Benıtez et al., 2020; Leming et al., 2020; Sorensen et al., 2020). Adeli and colleagues have employed deep neural network learning algorithms for the solution of various complicated pattern recognition and data mining problems such as concrete mixed design (Rafiei et al., 2017a) and estimation of concrete compressive strength (Rafiei et al., 2017b). A novel work on ML-aided global and local health condition assessment of structures, structural integrity, and health monitoring has been recently published (Rafiei & Adeli, 2018).

An early example of health monitoring of steel structures is the work of Hampshire and Adeli (2000) who used distributed optical fiber sensors to monitor the behavior of steel structures. An early important work on the application of ML in structural health monitoring employing a multi-paradigm approach is the MUSIC and dynamic wavelet neural network model for damage detection of high-rise buildings (X. Jiang & Adeli, 2007). Park et al. (2007) introduced terrestrial laser scanning as a new approach for health monitoring of structures. A review of articles on SHM up to 2014 was presented by Qarib and Adeli (2014), feature extraction and classification techniques for SHM were presented by Amezquita-Sanchez and Adeli (2015), and signal processing techniques for SHM by Amezquita-Sanchez and Adeli (2016). Oh et al. (2017) presented an evolutionary learning-based strain sensing model for SHM of high-rise buildings.

Among the most recent work, N. Wang et al. (2020) presented damage segmentation and measurement of

glazed tiles in historic buildings using deep learning. Yu and Zhang (2020) describe a feature tracing algorithm for bridge deflection monitoring. M. Wang and Cheng (2020) discussed a convolutional neural network (CNN) integrated with a conditional random field for pipe defect segmentation. Deng et al. (2020) also discussed concrete crack detection with handwriting script interferences using CNN. S. Jiang and Zhang (2020) described real-time crack assessment using deep learning with a wall-climbing unmanned aerial system. J. Liu et al. (2020) presented automated pavement crack detection and segmentation using CNN. Other recent developments on ML methods for structural health monitoring have been published by Athanasiou et al. (2020) and Zhang and Aoki (2020).

1.2 | Deterministic fatigue damage-based methods

Available fatigue models for damage accumulation estimation and life prediction can only be applied on cyclic loading histories. Since the loading on structures under environmental conditions (wind, wave, earthquake, etc.) has random nature, the first step for deterministic fatigue-based estimation of damage accumulation and life prediction is the transformation of the irregular loading history into a history containing loading cycles. The second step is the calculation of the fatigue damage of each loading cycle and the summation of the finite amounts of damage of each cycle.

For the first step, four transformations (or cycle counting) algorithms, namely, level-crossing counting, peak counting, range counting, and rainflow counting, have been proposed for fatigue life prediction (ASTM, 2011). Most of the counting algorithms do not have a solid physical base. Among them, the rainflow counting algorithm (Matsuishi & Endo, 1968; Richards et al., 1974) seems to provide the most accurate results (Carpinteri et al., 2017) because it composes loading cycles that correspond to closed stress-strain hysteresis loops. Although considerable progress has been achieved in damage models for uniaxial (Pavlou, 2018) and multiaxial (Carpinteri & Spagnoli, 2001) fatigue, the life prediction with all the available applicable methods is still based on the rainflow cycle counting (Matsubara & Hayashida, 2021; Pham et al., 2021; Stellmach et al., 2021; Xie et al., 2021). Rainflow algorithms are also used for the prediction of an equivalent number of cycles during an earthquake (Stafford & Bommer, 2009). Since the area of closed stress-strain hysteresis loops expresses the energy consumption for causing fatigue damage in the material structure, they can be considered as damage events. However, there is not a unique process for counting closed stress-strain hysteresis loops. The original version of rainflow method can be implemented via a complicated algorithm that counts the cycles as routes of raindrops on the roof of a pagoda that has the profile of the loading history (Figure 2). Therefore, it demands big computer core storage when it is applied to long loading histories. The several variations of the rainflow method have variable complexity but yield comparable results.

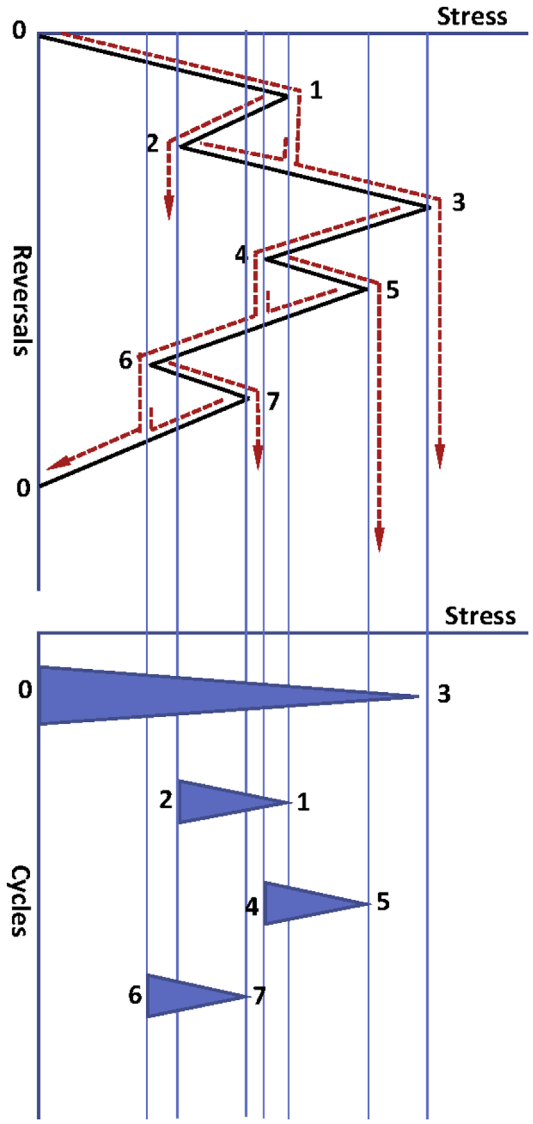

FIGURE 2 The tracks of the raindrops (dotted lines) in the irregular loading history compose the full loading cycles 0-3-0, 2-1-2, 4-5-4, and 6-7-6

The second step in damage accumulation simulation is carried out with the aid of a linear or several nonlinear fatigue damage summation models. The linear model, known as Miner's rule (Miner, 1945), is used in all structural design codes American Institute of Steel Construction ((AISC), Eurocode, DNV-GL, etc.) because of its simplicity. However, it is inconsistent with the nonlinear material mechanisms during fatigue. For this

reason, it cannot consider the load interaction effects in damage accumulation.

Although the design codes have adopted only Miner's uniaxial fatigue model, the fatigue life prediction under multiaxial loads is usually carried out by fatigue criteria for the transition from multiaxial stress state to equivalent uniaxial one (Macha & Niesłony, 2012). On the derived equivalent uniaxial stress histories, the rainflow cycle counting and Miner's linear summation are applied. Pioneering works on multiaxial fatigue have been published by Carpinteri and Spagnoli (2001), Carpinteri et al. (2015), Fatemi and Socie (1988), Sharifimehr and Fatemi (2019), and Papadopoulos (1994). A recent review of multiaxial fatigue models can be found in Dantas et al. (2021).

An alternative approach for fatigue life prediction estimation is based on frequency-domain fatigue-based methods (e.g., Yue et al., 2021). This approach uses a variation of Miner's linear rule and can be used for a quick approximation of the fatigue life. It is usually adopted for the preliminary design of steel structures.

Apart from Miner's linear rule, several nonlinear damage models have been published in the last decades. Popular models of the period 1975–2005 have been published by Hashin and Rotem (1978), Pavlou (2002), Subramanyan (1976), and so forth. The most recent models can be found in the publications of Q. Liu et al. (2020), Pavlou (2018), Aeran et al. (2017), Rege and Pavlou (2017), Si-Jian et al. (2018), and Theil (2016). The nonlinear models are grouped into several categories (Fatemi & Yang, 1998): two-stage linear models, life curve modification models, models based on the crack growth process, continuum damage mechanics models, and energy-based models. Two detailed reviews of the most important fatigue damage accumulation models have recently been published by Hectors & De Waele (2021) and Zhu, Hao, et al. (2019). Further relevant works on fatigue damage accumulation have been published by Correia et al. (2017), X. Liu et al. (2019), Zhu, Liao, et al. (2019), Zhu et al. (2018), Horas et al. (2017), and so forth.

The functional form of the nonlinear fatigue damage models for a constant amplitude loading with stress amplitude σ is the following:

$$D = \left(\frac{n}{N(\sigma)}\right)^{q(\sigma)} \tag{1}$$

where D is the damage function taking values from $D =$ 0for undamaged material to $D = 1$ for material failure, $q(\sigma)$ is a function of the stress amplitude, n is the number of the applied loading cycles, and $N(\sigma)$ is the life (in loading cycles) corresponding to stress amplitude σ. The stress life function $N(\sigma)$ can be obtained by the experimentally derived S-N curves. Application of a nonlinear model to a structure subjected to multi-stage stepwise constant amplitude loading (Hectors & De Waele, 2021) yields:

$$D = \left\{\left\{\cdots\left\{\left(\left(\frac{n_1}{N_{f1}}\right)^{\frac{q(\sigma_2)}{q(\sigma_1)}} + \frac{n_2}{N_{f2}}\right)^{\frac{q(\sigma_3)}{q(\sigma_2)}} + \frac{n_3}{N_{f3}}\right\}^{\frac{q(\sigma_4)}{q(\sigma_3)}} + \cdots + \frac{n_{N-1}}{N_{f(N-1)}}\right\}^{\frac{q(\sigma_N)}{q(\sigma_{N-1})}} + \frac{n_N}{N_{f(N)}}\right\}^{\frac{1}{q(\sigma_N)}} \tag{2}$$

Although the nonlinear models are advantageous because they take into account the loading sequence effects, none of them has been adopted by the design codes because of their complexity. Due to the repeated exponential damage summation in thousands loading cycles (Equation 2), the accumulated numerical error is very large and the application on real loading spectra is useless. Only results on simple two-stage until four-stage stepwise constant amplitude loadings are available. In most of the published research, only ratios of exponents $q(\sigma_i)/q(\sigma_{i-1})$ exist. Only in the works of Rege and Pavlou (2017) and Pavlou (2002), the models containing full function $q(\sigma)$ can be found, but the verification of these models has also been carried out in two-stage stepwise constant loadings.

In the present work, a new algorithm for nonlinear fatigue damage accumulation estimation on structures under spectrum loading is proposed. The algorithm contains two tools: a new cycle counting algorithm and a new damage summation method. The proposed counting algorithm inserts suitable fictitious full loading cycles on an irregular spectrum loading and transforms it into a substitute loading history that contains full loading cycles. Obviously, the substitute loading history includes the damage effect of both the original spectrum loading and the fictitious loading cycles. The damage of the substitute

history and the damage of the inserted fictitious cycles can be calculated because their loads are cyclic. The damage of the original spectrum loading can be obtained by the compensation of the calculated damages of the loading cycles of the substitute history and the fictitious ones. The proposed damage summation method is based on the multilinear transformation of the nonlinear damage accumulation model. This approach is advantageous because it preserves the applicability of the linear summation (within the finite linear damage bands) and performs nonlinear damage summation with the aid of weighting functions. With the proposed algorithmic tools, nonlinear damage accumulation estimation on spectrum loading is carried out for the first time. The method has five advantages: (a) It takes into account the loading sequence effect in fatigue damage accumulation estimation, (b) it provides applicable nonlinear damage summation, (c) it is consistent with the nonlinear material mechanisms during fatigue, (d) it can be used for reliable fatigue life prediction in structures under spectrum loading, (e) it can be used for developing reliable inspection plans (shorter inspection intervals when the damage accumulation rate is high), (e) it can be used for real-time structural health monitoring. Because of the lack of environmental loads, a random generation command in Wolfram Mathematica is used for generating spectrum loadings. Implementation of the proposed algorithm is carried out in various types of random loading, that is, high-low two-stage random loading, low-high two-stage random loading, decreasing amplitude multi-stage random loading, increasing amplitude multi-stage random loading, and alternating amplitude random loading. The obtained results are compared with results from the existing standard method of the rainflow counting algorithm and Miner's linear damage summation. From the derived results, important conclusions about the loading sequence effect on fatigue damage accumulation are obtained.

2 | THE NEW COUNTING ALGORITHM

The idea behind the new algorithm is to add proper fictitious discrete loading cycles (Figure 3b) in the irregular history (Figure 3a) that can transform it into a regular (substitute) one (Figure 3c), and then to remove the effect of the added fictitious cycles from the cycles of the substitute cyclic history.

The proposed algorithm is described in Figure 4. For the sake of simplicity, the transformation steps are applied to the elementary irregular history of Figure 4a. The selected loading history in Figure 4a does not contain loading cycles, and direct implementation of fatigue models is impossible.

From the physical point of view, the corresponding stress-strain diagram in Figure 4a includes three closed stress-strain hysteresis loops (Figure 4b). Since the strain energy within the area of each hysteresis loop is irreversible and causes deterioration in the material microstructure, it is considered a damaging event. Therefore, in Figure 4b, three damaging events can be counted: loop σ_2-σ_1, loop σ_0-σ_3, and loop σ_4-σ_5. The corresponding loading cycles σ_2-σ_1-σ_2, σ_0-σ_3-σ_0, and σ_4-σ_5-σ_4 in Figure 4c can approximately cause the same fatigue damage as the irregular loading history in Figure 4a. Although this physical process for loading cycle counting is reasonable, the integration of the hysteresis loops cannot be applied in real service loading histories that usually contain millions of loading reversals. In engineering practice, it is not possible to record the stress-strain hysteresis loops of structures. The rainflow algorithm is a valuable tool for loading cycles counting but the process of the routes of raindrops on a pagoda roof with an irregular profile is complicated and requires a large computer storage capacity. On the other hand, the linear damage summation of the derived cycles neglects the loading sequence effect. An alternative, much simpler algorithm, which counts loading cycles based on loading loops, is demonstrated in Figures 4d–g. On the valleys of the original loading history, we add the fictitious loading cycles σ_2-σ_0-σ_2 and σ_4-σ_0-σ_4 (Figure 4d). The obtained loading history σ_0-σ_1-σ_0-σ_3-σ_0-σ_5-σ_0 is not irregular anymore, but the corresponding fatigue damage is larger than the fatigue damage of the original irregular history because it includes the damage of the fictitious loading cycles. Figure 4e demonstrates the counted damaging events of the cyclic loading history of Figure 4d that include the damaging events of the fictitious cycles signed by "–," that is, it includes the fictious damaging events. Then, the fictitious damaging events are deducted (Figure 4f) from the substitute cyclic history, yielding the damaging events in Figure 4g. It is obvious that the corresponding loading cycles of the damaging events of the Figure 4g are same as the loading cycles in Figure 4c counted by the stress-strain loops of Figure 4b. In order to get the above results, the deduction of the fictious damaging events should follow the following rules:

If the stress σ_j^{υ} of any valley $j$of the original loading history fulfills the condition

$$\left|\sigma_{j+1}^{\max} - \sigma_j^{\upsilon}\right| > \left|\sigma_{j-1}^{\max} - \sigma_j^{\upsilon}\right| \tag{3}$$

then the fictitious damaging event is deducted from the damaging event of the stress $\sigma_{j-1}^{\max}$, and the resulted loading cycle has maximum stress $\sigma_{j-1}^{\max}$ and minimum stress $\sigma_{j-1}^{\min} = \sigma_j^{\upsilon}$ (Figure 5a):

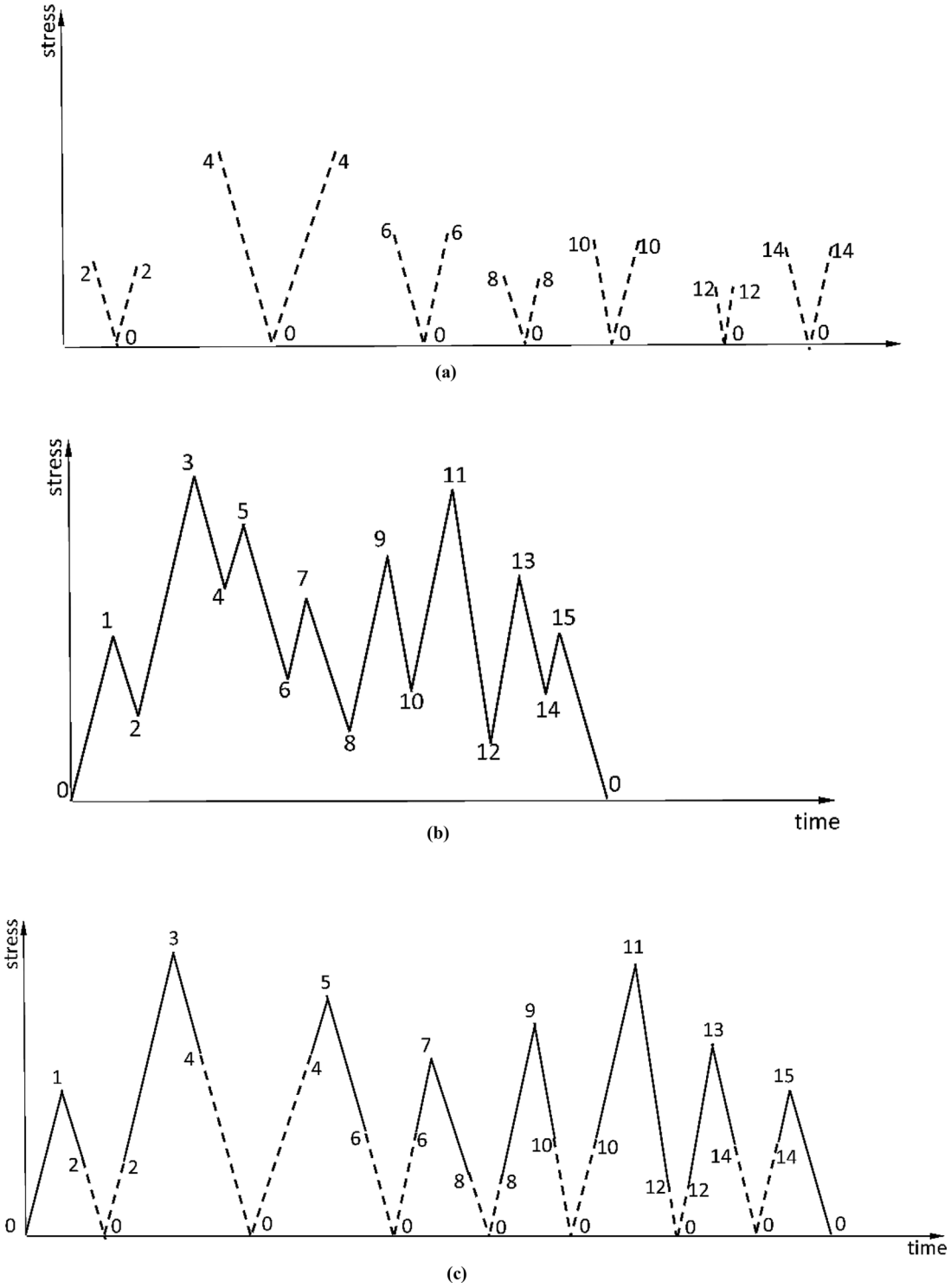

FIGURE 3 (a) Irregular loading history, (b) fictitious cycles, and (c) substitute cyclic loading history physical

If

$$\left|\sigma_{j+1}^{\max} - \sigma_j^{v}\right| < \left|\sigma_{j-1}^{\max} - \sigma_j^{v}\right| \tag{4}$$

the fictitious damaging event is deducted by the damaging event of the stress $\sigma_{j+1}^{\max}$, yielding a loading cycle with maximum stress $\sigma_{j+1}^{\max}$ and minimum stress $\sigma_{j+1}^{\min} = \sigma_j^{v}$ (Figure 5b). For stress peaks and valleys in the compressive area, the same procedure can be applied (Figure 6). The real service spectra usually contain knee points and plateaus that should be removed before the implementation of the proposed algorithm. Since the mean stress σ_m of

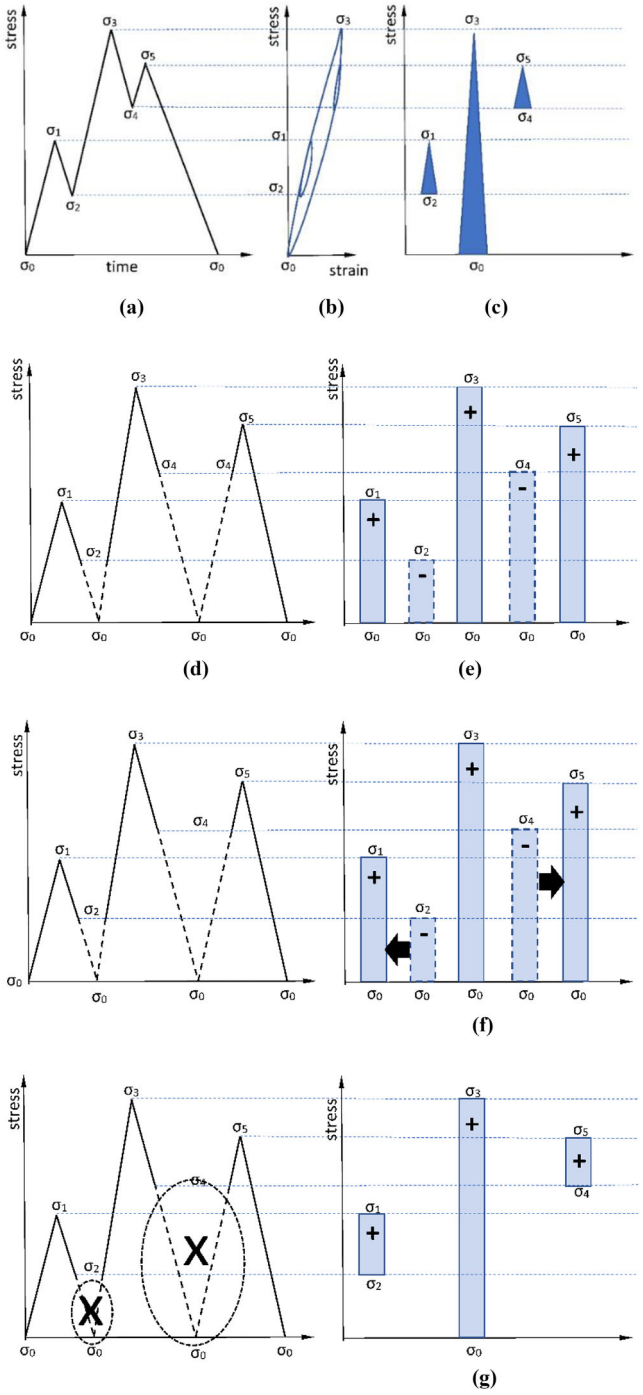

FIGURE 4 (a) Elementary irregular loading history, (b) stress-strain hysteresis loops, (c) loading cycles corresponding to the stress-strain hysteresis loops, (d) insertion fictitious loading cycles into an irregular spectrum, (e) loading cycles of the substitute loading history (continue line) and fictitious loading cycles (dotted line), (f) compensation of the loading cycles of the substitute history and the fictitious loading cycles, and (g) derived loading cycles equivalent to the original loading history

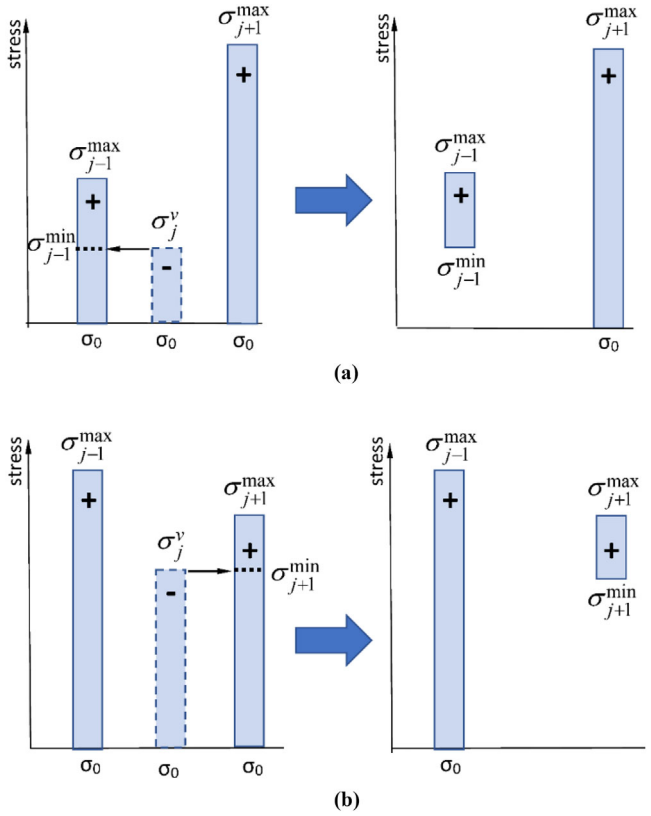

FIGURE 5 Rules for deduction the fictitious damaging events from the substitute loading history: (a) increasing successive stress peaks in the original spectrum, and (b) decreasing successive stress peaks in the original spectrum

the majority of the derived loading cycles is $\sigma_m \neq 0$, equivalent stress amplitudes should be calculated in order to consider the mean stress effect. To this end, well-known mean stress effect rules like, for example, Goodman's can be implemented:

$$\frac{\Delta\sigma_i}{\Delta\sigma_i^{eq}} + \frac{\sigma_i^{mean}}{S_u} = 1 \tag{5}$$

After the implementation of the algorithm, a huge number of cycles with stress amplitude $\Delta\sigma^{eq}$ less than the fatigue endurance limit S_e exist. These loading cycles should be removed because they do not contribute to the damage accumulation. In the obtained loading history, which contains discrete loading cycles, a fatigue damage accumulation model should be applied. Linear models do not take into account the loading sequence effects. It is well known that the reason of the loading sequence effects is the plastic zone sizes produced by the maximum values of the

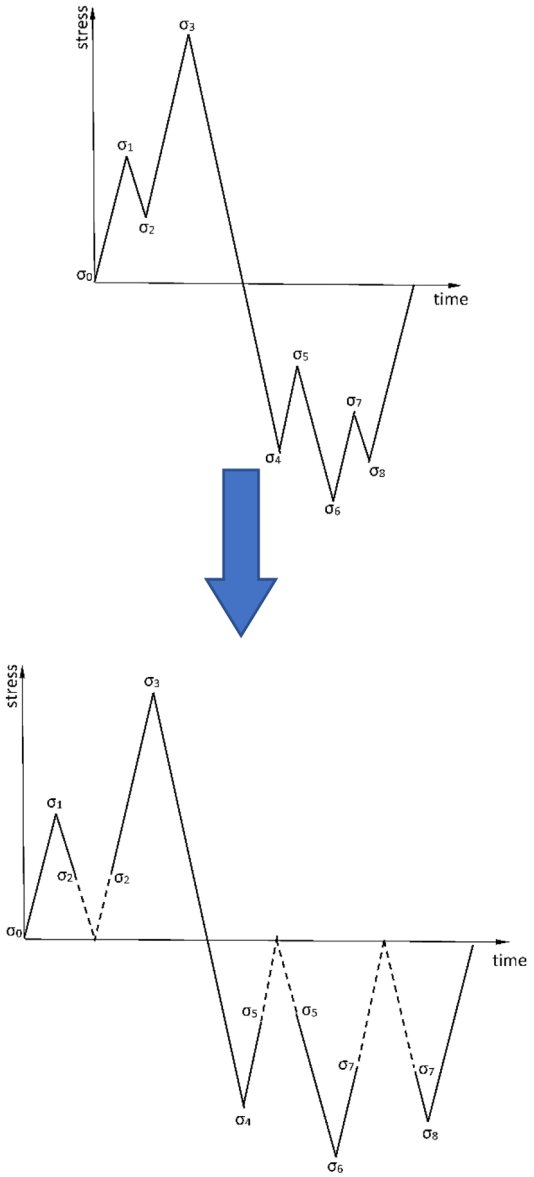

FIGURE 6 Fictitious loading cycles in loading histories with compressive stress peaks and valleys

stress sequence. Therefore, for nonlinear damage accumulation prediction, the sequence of the derived discrete loading cycles should follow the sequence of the stress peaks of the original loading history. All the above steps for the transformation of an irregular loading history into a history containing loading cycles is demonstrated in the flow chart of Figure 7.

2.1 | Comparison with the rainflow counting method

All the published counting methods are based on the assumption that the surface of the closed stress-strain hysteresis loop expresses the consumed mechanical energy to cause fatigue damage in a material structure. However, they do not count the surface of the closed hysteresis loops but the stress range composing loading loops. Since the real-time surface integration of hysteresis loops during service is practically impossible, this approach, though approximate, is useful due to its simplicity. Furthermore, it yields acceptable results for engineering purposes. The stress range is not a sufficient parameter to measure the area of a closed stress-strain hysteresis loop. The hardening exponent, the mean stress, the strain rate, and the temperature are additional necessary parameters that should be accounted for the estimation of the mechanical energy causing fatigue damage in the material structure. Therefore, all the known counting methods count closed loading loops, not closed hysteresis loops. Since the creation of a closed loading loop by assembling several loading reversals from different places of the loading history is not unique and straightforward, the several counting methods count different loading cycles. The existing four concepts and their variations are based on different algorithms that differ in complexity. The selection of a counting algorithm is a compromise of the computational cost and the required accuracy. It seems that rainflow method yields the most accurate results but the corresponding algorithm of composing cycles from the tracks of rain drops (Figure 2) is the most complicated. The rainflow method is considered the standard counting method in fatigue design packages and structural health monitoring systems and has been adopted by most of the design standards.

The proposed counting algorithm of inserting fictitious loads to transform an irregular spectrum to a cyclic one counts loading cycles that correspond to closed loading loops too. In most of the irregular loading patterns, like in Figure 4a, the proposed algorithm, though much simpler, counts the same loading cycles as the rainflow method. However, in few loading patterns, the existing counting algorithm and the rainflow count different closed loading loops (Figure 8a,b).

If we assume that the area within a closed stress-strain hysteresis loop is proportional to the stress range $\Delta\sigma = \sigma_{max} - \sigma_{min}$, the sum of the derived stress ranges by rainflow $(\sigma 1 - \sigma 0) + (\sigma 3 - \sigma 4) + (\sigma 5 - \sigma 2)$ in Figure 8a is equal to the sum of the derived stress ranges by the proposed method $(\sigma 1 - \sigma 0) + (\sigma 3 - \sigma 2) + (\sigma 5 - \sigma 4)$ in Figure 8b.

3 | THE NEW DAMAGE SUMMATION ALGORITHM (MULTILINEAR DAMAGE SUMMATION)

The last module in the algorithm in Figure 7 contains the damage summation algorithm. The structural design codes

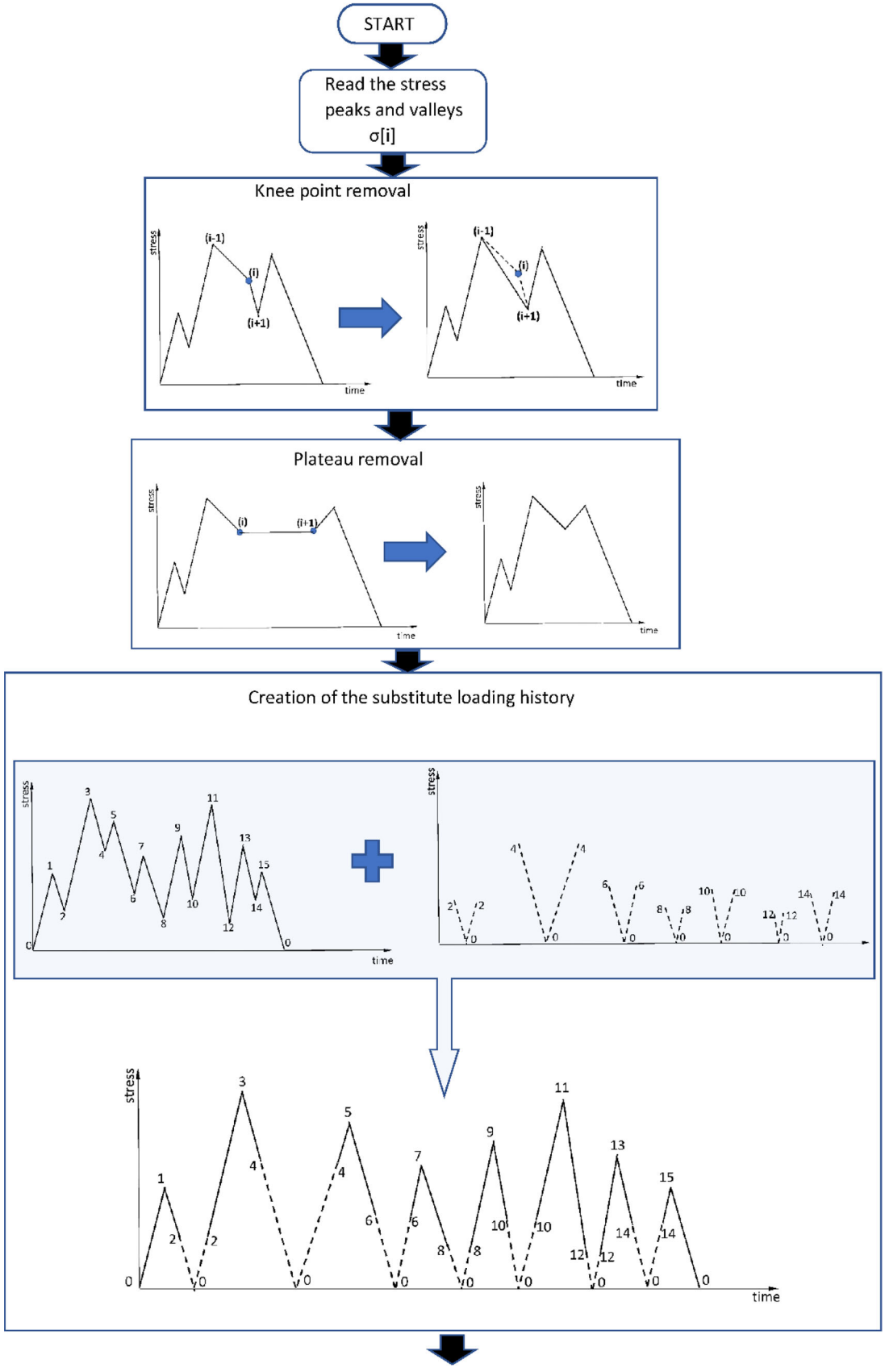

FIGURE 7 Proposed concept for cycle counting algorithm

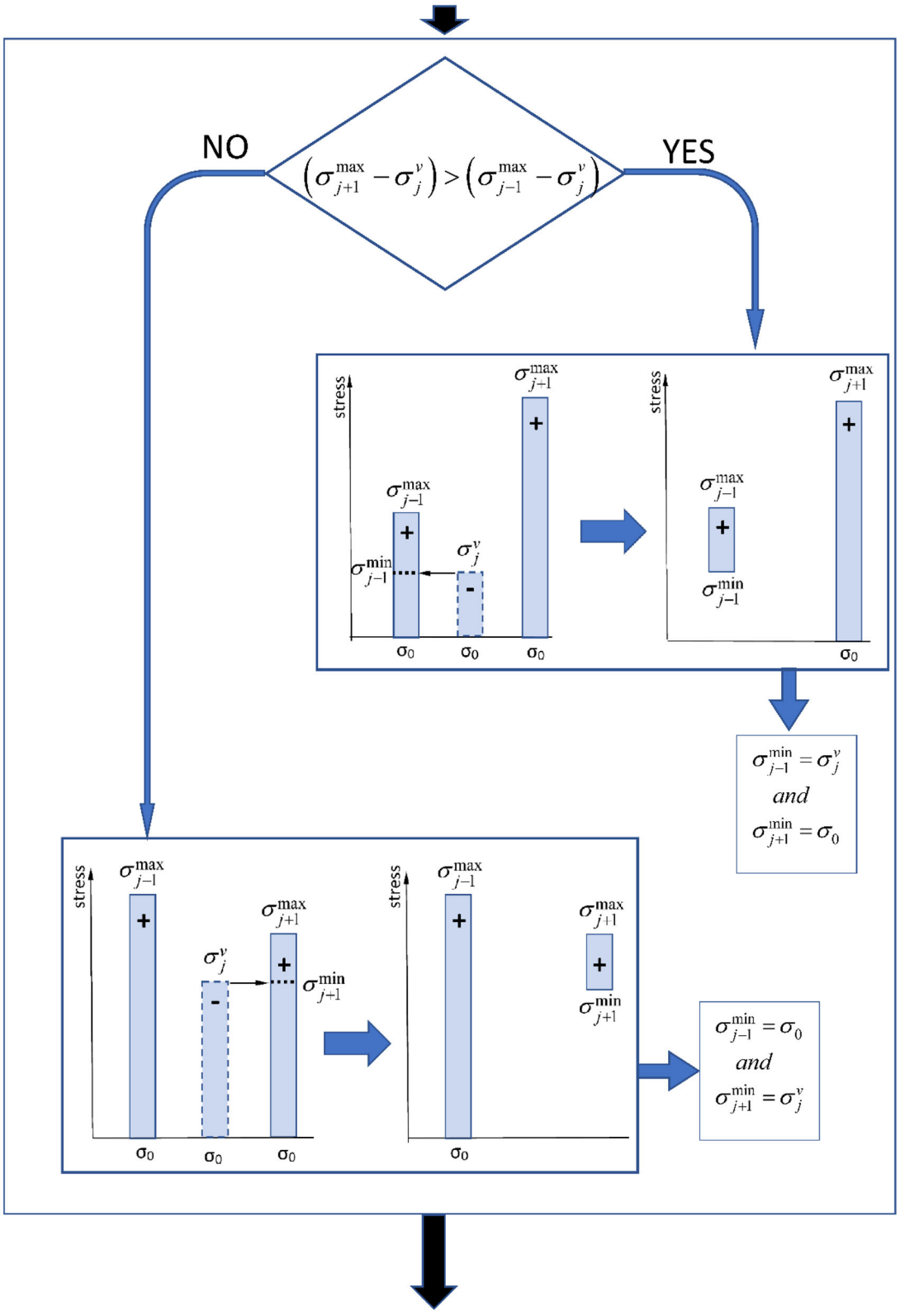

FIGURE 7 Continued

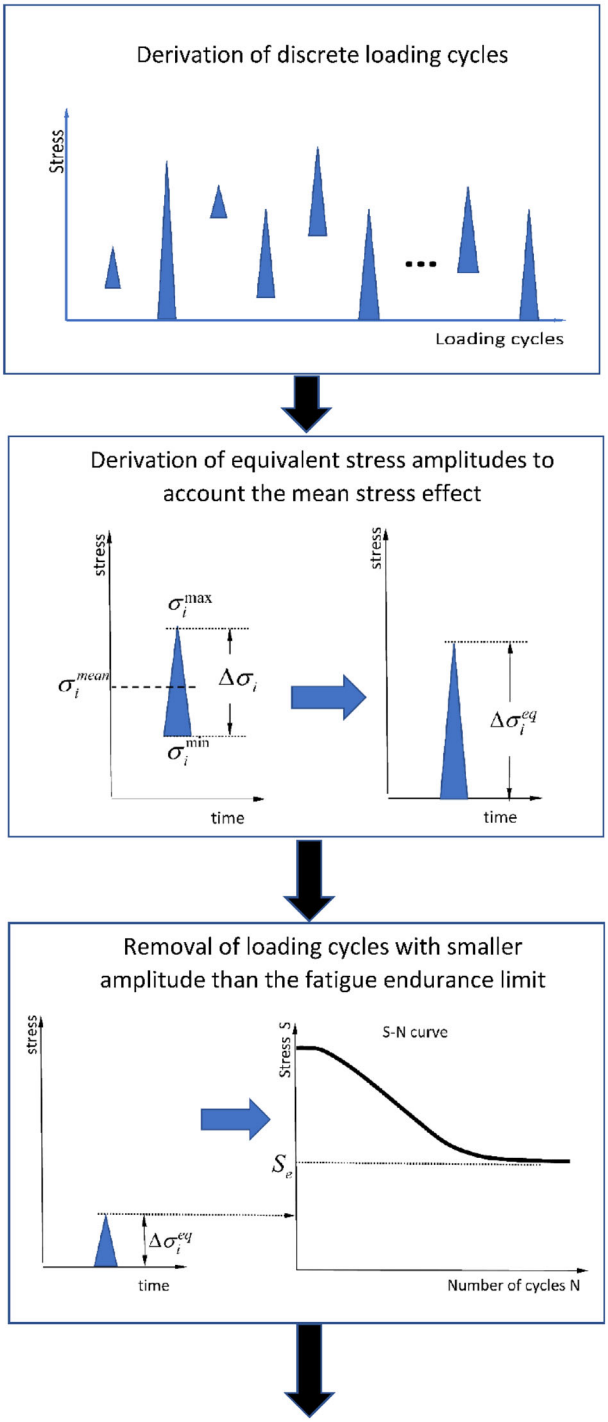

FIGURE 7 Continued

(AISC, Eurocode, DNV-GL etc.) use the Miner's linear rule because of its simplicity. Although the available nonlinear models provide a realistic simulation of the fatigue damage accumulation and take into account the loading sequence effect, they cannot be applied to irregular loading spectra because the repeated exponents on exponents in Equation (2) yields a very large error even for few tens of loading cycles.

To overcome these disadvantages, the discretization of the nonlinear damage evolution into finite multi-stress damage bands where the damage curves can be approximated by linear segments with different slopes is proposed herein. Within the multilinear iso-stress damage curves that preserve the damage memory of the material, linear damage summation can be performed.

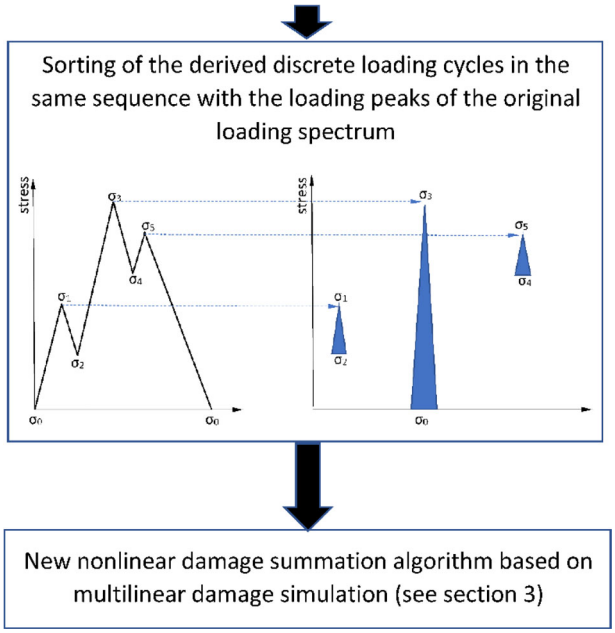

FIGURE 7 Continued

Any point within the area of a damage envelope correlates with three parameters: Damage function D, stress amplitude σ, and normalized number of loading cycles $n^* = n/N$ (Figure 9).

During the service life of a real structure, a very large number of stress reversals composes the stress history. The damage increment due to a single loading cycle has an extremely small value. For estimation of the total damage accumulation, the non-linear summation of an extremely large number of damage increments of the loading cycles composing the loading spectrum should be carried out. Since even small differences always exist between the actual values and the calculated ones of the damage increment, direct implementation of the Equation (2) to million loading cycles yields error accumulation and inaccurate results.

In order to minimize the numerical error, the diagram of the damage evolution (Figure 9) is divided into damage bands (Figure 10). To each damage band, straight segments approximate the curved damage lines (iso-stress curves). Each straight segment has a certain slope, expressing the corresponding damage accumulation rate within the corresponding damage band (Figure 11). The slope of each straight line represents the material memory of the damage accumulation in the past.

The size of the bands is arbitrary, like the size of the finite differences and finite elements in structural analysis. More bands result in better accuracy. Dense discretization of the envelope at the early stage of fatigue damage accumulation (e.g., in the area $D < 0.1$) is a good practice. An optimization for determining the band height can be carried out but it is beyond the scope of the present work. The minimum for the number of bands is 2. The damage increment ΔD due to a small number of loading cycles $\Delta n/N$ with a certain stress amplitude σ_i is:

$$\Delta D = \frac{\Delta n}{N} \tan \varphi_i \tag{6}$$

where φ_i is the slope of the straight segment corresponding to the stress amplitude σ_i in a certain damage band.

According to Miner's rule, the damage increment ΔD_M for the same normalized number of loading cycles $\Delta n\ /N$ is

$$\Delta D_M = \frac{\Delta n}{N} \tan 45^o \tag{7}$$

Then, the combination of Equations (6) and (7) yields:

$$\Delta D = \frac{\tan \varphi_i}{\tan 45} \Delta D_M \tag{8}$$

Taking into account the above equation, the ratio

$$w_i = \frac{\tan \varphi_i}{\tan 45} \tag{9}$$

can be considered as a weight coefficient for correction of the Miner's damage calculation ΔD_M within a damage band. Therefore, within a certain finite damage band j, the damage summation ΔD_j can be performed linearly by using the weight coefficients w_{ij} of the stresses i within the

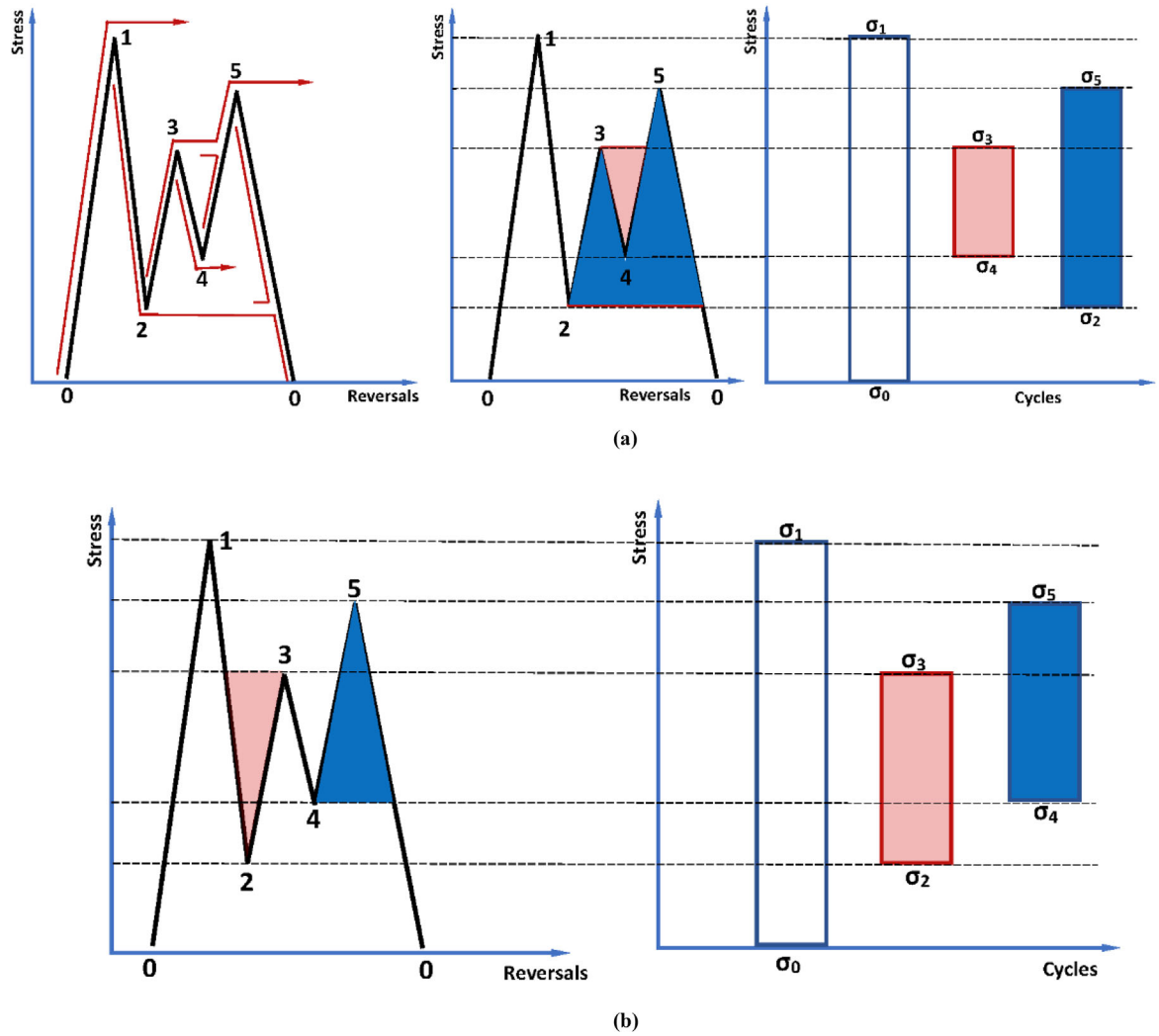

FIGURE 8 (a) Rainflow algorithm counted the closed loading loops σ0-σ1-σ0, σ4-σ3-σ4 and σ2-σ5-σ2, (b) the proposed algorithm counted the closed loading loops σ0-σ1-σ0, σ2-σ3-σ2 and σ4-σ5-σ4

damage band j:

$$\Delta D_j = \sum_{i=1}^{k} w_{ij} \frac{n_i}{N_i} = w_{1j}\frac{n_1}{N_1} + w_{2j}\frac{n_2}{N_2} + \cdots + w_{kj}\frac{n_k}{N_k} \tag{10}$$

The total damage can be calculated by the summation of damage increments of all damage bands

$$D = \sum_{j=1}^{nb} \Delta D_j \tag{11}$$

or

$$D = \sum_{j}^{nb} D_j = \sum_{j}^{nb} \sum_{i=1}^{k} w_{ij} \frac{n_i}{N_i} \tag{12}$$

where nb is the selected number of bands. With the aid of Equation (1), the weight coefficient w_{ij} can be derived by the following formula:

$$w_{ij} = \frac{D_j - D_{j-1}}{D_j^{1/q(\sigma_i)} - D_{j-1}^{1/q(\sigma_i)}} \tag{13}$$

Using the above concept, the damage summation within a band can be considered linear. The damage memory of the material is taken into account by the use of the weights w_{ij}. Therefore, although the damage accumulation within a damage band is linear, the actual damage accumulation estimation for the whole stress history is non-linear. The proposed method is summarized in a pseudocode listed in the Appendix.

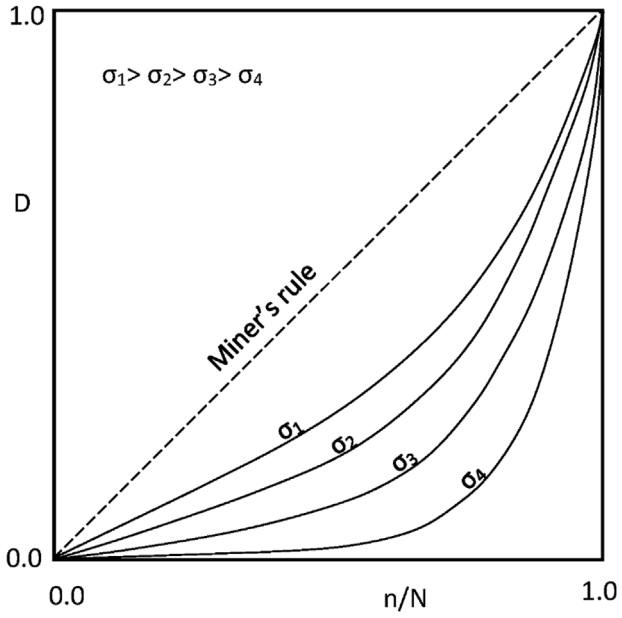

FIGURE 9 Schematic representation of the damage D versus the normalized number of cycles n/N for several values of stress amplitude σ (iso-stress curves)

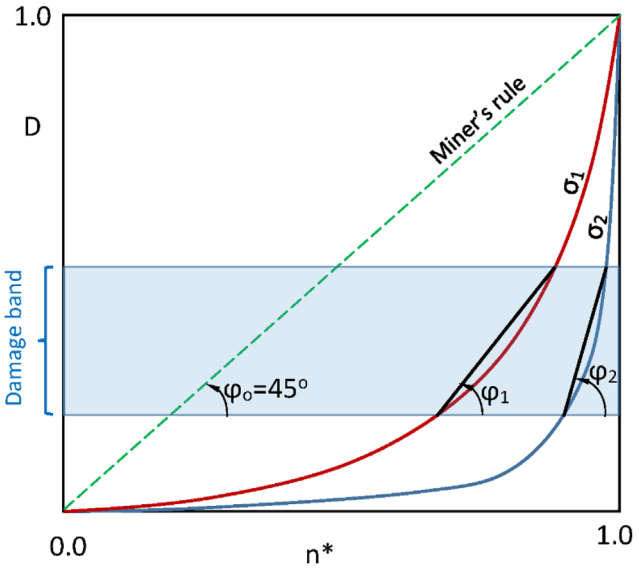

FIGURE 11 Approximation of the continuous damage accumulation curves of each band by straight segments with a constant slope

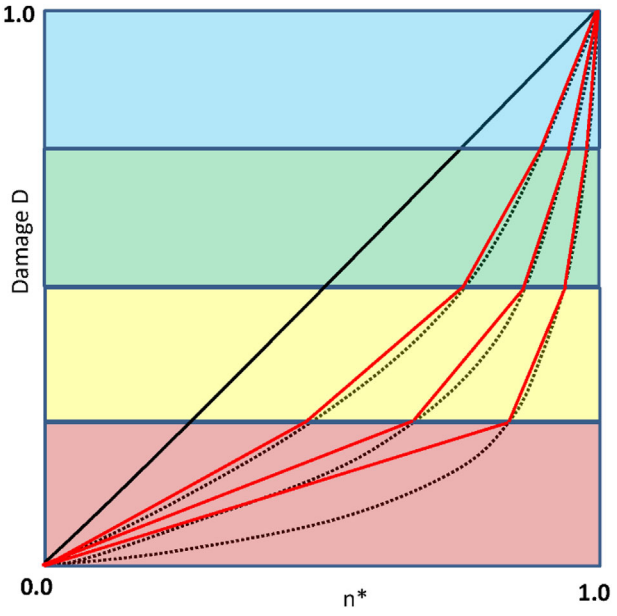

FIGURE 10 Discretization of the damage accumulation curves into four bands

4 | IMPLEMENTATION OF THE PROPOSED ALGORITHM TO AN OFFSHORE WIND TURBINE STRUCTURE

Real-time structural health monitoring of offshore wind turbine structures is based on loading series recordings on critical spots of the structure. Typical load recordings are the blade bending and torsion moments, both at the blade root and the monopile base. The fatigue loads have harmonic (wave inputs) and stochastic (wind inputs) components (Figure 12).

With the aid of numerical methods, the loading series recordings are transformed into stress series for each critical spot. Since many critical locations exist, a huge volume of stress values due to the environmental loads are obtained. The stress spectra are irregular; therefore, an initial filtering for knee point and plateau removal is carried out first. Then a counting algorithm is applied, and a series of full loading cycles is derived for each stress spectrum. Equivalent stress amplitudes are calculated with the aid of multiaxial fatigue criteria and removal of loading cycles with smaller amplitude than the fatigue endurance limit is carried out. The remaining cyclic stresses are sorted in the same sequence with the stress peaks of the original stress spectrum. Finally, a damage summation algorithm is applied, and damage accumulation estimation is carried out.

Because of the lack of environmental stress series, a generation of random stress values with the aid of Mathematica is carried out for the sake of application of the proposed algorithm. Several loading scenarios are selected in order to examine the corresponding loading sequence effects. For the sake of calculations, a typical S-N diagram for steels is used (Figure 13) according to DNV-GL (2015) standards for S-N curve extrapolation for offshore structures. For the implementation of the proposed multilinear damage summation, the iso-stress family of the damage curves is discretized into $nb = 11$ damage bands. For better accuracy in the damage accumulation estimation, the discretization

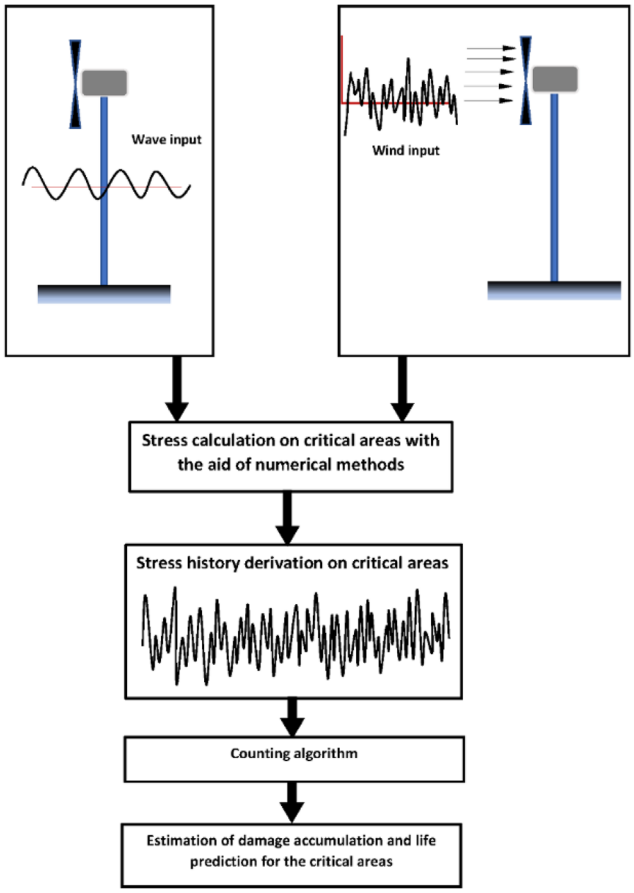

FIGURE 12 Real-time structural health monitoring for critical spots

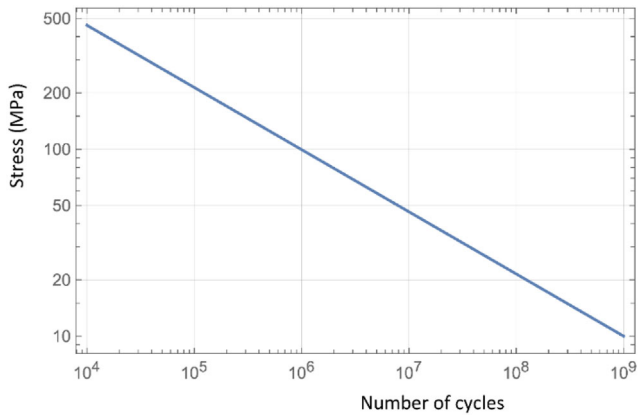

FIGURE 13 S-N curve

is denser at the early stage of the fatigue damage accumulation period, that is, for $D < 0.1$ where the material consumes most of its fatigue life. Optimization of the discretization of the damage envelope is beyond the aims of the present work. The formula for the weight coefficient for the 11 damage bands is:

$$w_{ij} = \begin{cases} \dfrac{0.025}{0.025^{1/q(\sigma_i)}} & \text{for } D \le 0.025 \\ \dfrac{0.05-0.025}{0.05^{1/q(\sigma_i)}-0.025^{1/q(\sigma_i)}} & \text{for } 0.025 < D \le 0.05 \\ \dfrac{0.1-0.05}{0.1^{1/q(\sigma_i)}-0.05^{1/q(\sigma_i)}} & \text{for } 0.05 < D \le 0.1 \\ \dfrac{0.2-0.1}{0.2^{1/q(\sigma_i)}-0.1^{1/q(\sigma_i)}} & \text{for } 0.1 < D \le 0.2 \\ \dfrac{0.3-0.2}{0.3^{1/q(\sigma_i)}-0.2^{1/q(\sigma_i)}} & \text{for } 0.2 < D \le 0.3 \\ \dfrac{0.4-0.3}{0.4^{1/q(\sigma_i)}-0.3^{1/q(\sigma_i)}} & \text{for } 0.3 < D \le 0.4 \\ \dfrac{0.5-0.4}{0.5^{1/q(\sigma_i)}-0.4^{1/q(\sigma_i)}} & \text{for } 0.4 < D \le 0.5 \\ \dfrac{0.6-0.5}{0.6^{1/q(\sigma_i)}-0.5^{1/q(\sigma_i)}} & \text{for } 0.5 < D \le 0.6 \\ \dfrac{0.7-0.6}{0.7^{1/q(\sigma_i)}-0.6^{1/q(\sigma_i)}} & \text{for } 0.6 < D \le 0.7 \\ \dfrac{0.8-0.7}{0.8^{1/q(\sigma_i)}-0.7^{1/q(\sigma_i)}} & \text{for } 0.7 < D \le 0.8 \\ \dfrac{1.0-0.8}{1.0^{1/q(\sigma_i)}-0.8^{1/q(\sigma_i)}} & \text{for } 0.8 < D \le 1.0 \end{cases} \tag{14}$$

For the exponent $q(\sigma_i)$ in the nonlinear damage function (Equation 1), the following formula (Rege & Pavlou, 2017) is adopted:

$$q(\sigma_i) = \left(\frac{\sigma_i}{Su}\right)^{-0.75} \tag{15}$$

where Su is the ultimate stress of the material. For the selected steel, the typical value $Su = 900$ MPa is used.

The first loading spectrum consists of a uniform block of random peaks and valleys in the range of values $\sigma \in [0,\ 500]$MPa (Figure 14a). The proposed algorithm yields the damage accumulation versus the number of cycles shown in Figure 14b. In the same figure, a plot of the damage accumulation curve derived by the rainflow counting and Miner's linear damage summation is included. The nonlinear damage accumulation nature is clearly demonstrated in the results of the proposed algorithm. For the selected random loading, the predicted fatigue life by the proposed algorithm is 29,735 cycles, while the predicted life by the rainflow counting and Miner's linear summation is 30,412 cycles. This result indicates that although the existing standard method is linear, the accuracy of the life prediction is excellent. The deviation of the predicted fatigue life with respect to the existing method is 2.23%. However, the existing method overestimates slightly the fatigue life. According to the author's opinion, the reason for the good agreement between the proposed nonlinear algorithm and

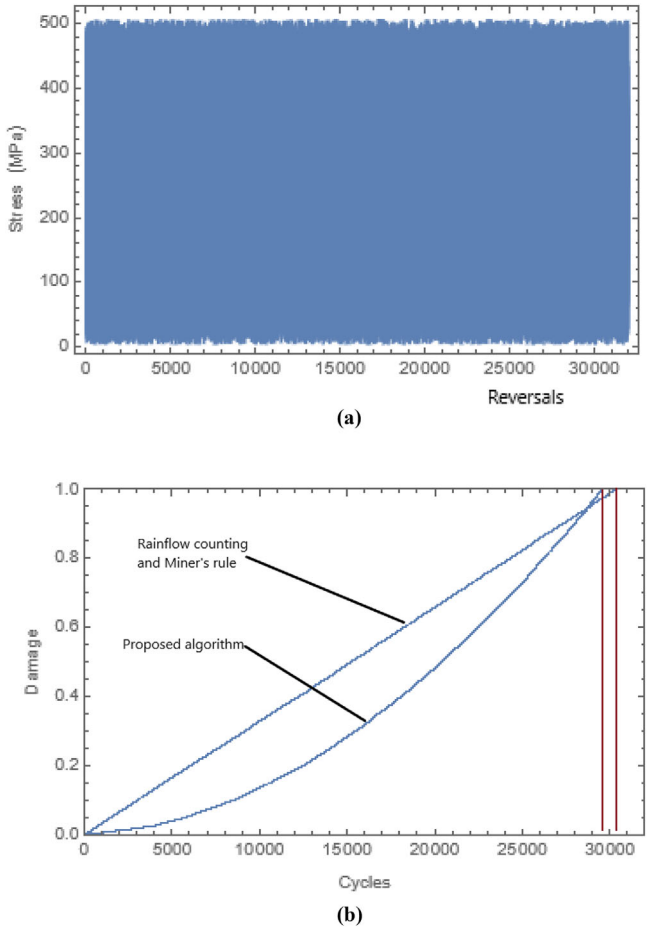

FIGURE 14 (a) Uniform random spectrum loading, (b) damage accumulation simulation and fatigue life prediction with the aid of the proposed and the existing method

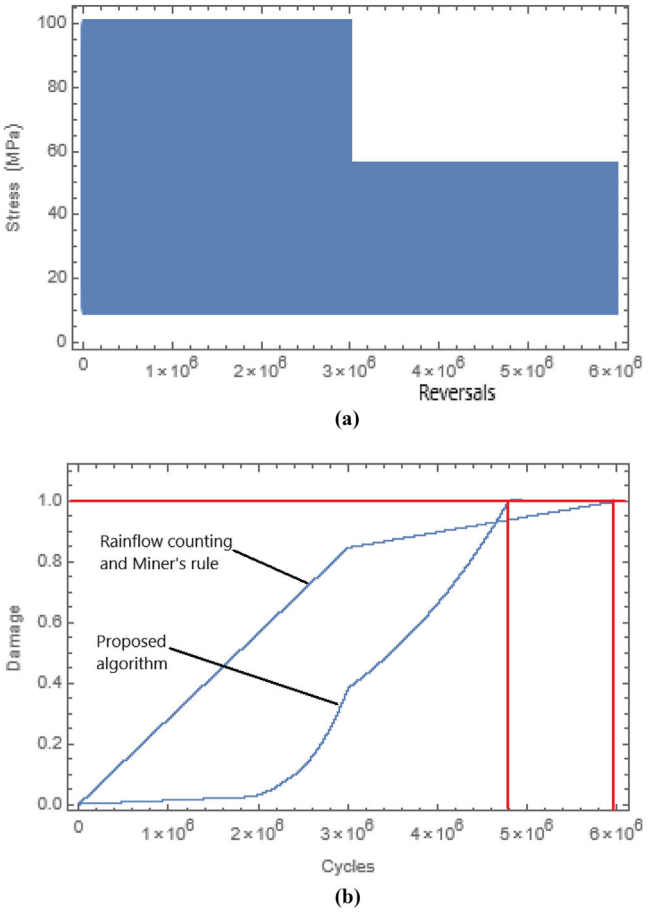

FIGURE 15 (a) High-low two-stage random loading, (b) damage accumulation simulation and fatigue life prediction with the aid of the proposed and the existing method

the existing linear is the fact that the effects of overloads and underloads cancel each other in a random loading history. Unlike this finding, the implementation of the proposed method to high-low two-stage random loading spectrum of Figure 15a resulted in large life prediction deviation between the proposed and the existing method. The results are demonstrated in Figure 15b and show that the existing method overestimates the fatigue life (deviation 18.77%). This finding indicates that ignoring the nonlinear nature of the damage accumulation yields inaccurate life prediction in loading spectra containing loading blocks of decreasing stress range. According to the results of this example, the loading sequence has a significant effect on the damage accumulation. The use of the existing method to loading spectra, which causes overloading of a structure at the early life, yields an unsafe prediction of the fatigue life and should be avoided. If we inverse the sequence (Figure 16a) of the loading blocks of the previous case, good agreement between the results of the proposed and the existing method is obtained (Figure 16b). The deviation between the predictions of the proposed and the existing method is just 1.43%. It seems the existing method underestimates slightly the fatigue life and can provide safe and slightly conservative results. Implementation of the model is carried out to multi-stage spectrum with decreasing random stress range (Figure 17a) and to multi-stage one with increasing random stress range (Figure 18a). The corresponding results are demonstrated in Figure 17b for the high to low multi-stage spectrum and in Figure 18b for the low to high one. These findings indicate the same trend like the results of the corresponding high-low and low-high two-stage loadings.

There is a large deviation of 59.16% between the results of the proposed and the existing method for the high to low multi-stage spectrum, and the existing method overestimates the fatigue life. Unlike this result, a good agreement (deviation 2.18%) between the life prediction of the proposed and the existing method for the low to high multi-stage spectrum is obtained, and the existing method underestimates slightly the fatigue life. Finally, the proposed method is implemented to multi-stage spectrum with alternating random stress range (Figure 19a).

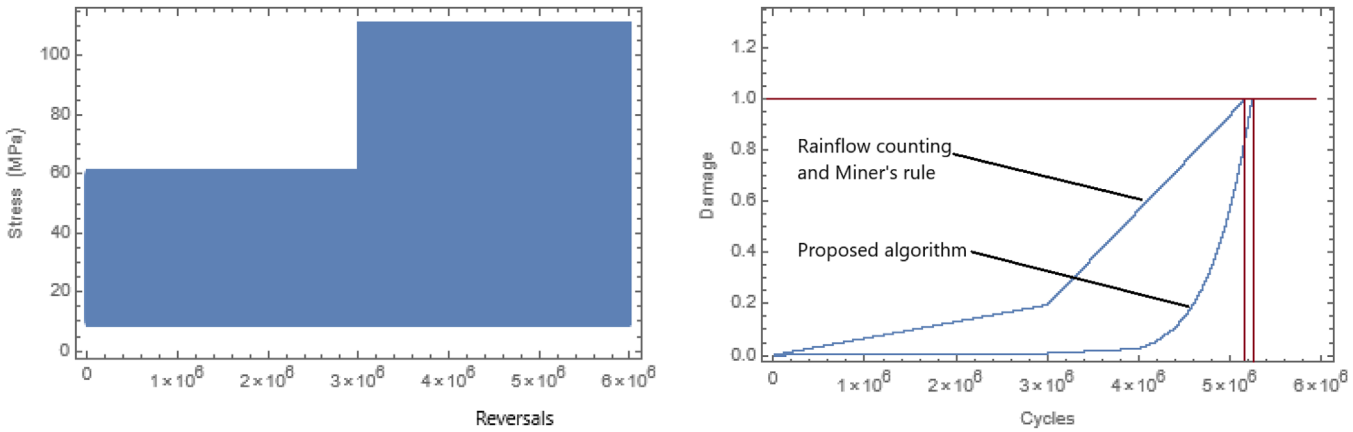

FIGURE 16 (a) Low-high two-stage random loading, (b) damage accumulation simulation and fatigue life prediction with the aid of the proposed and the existing method

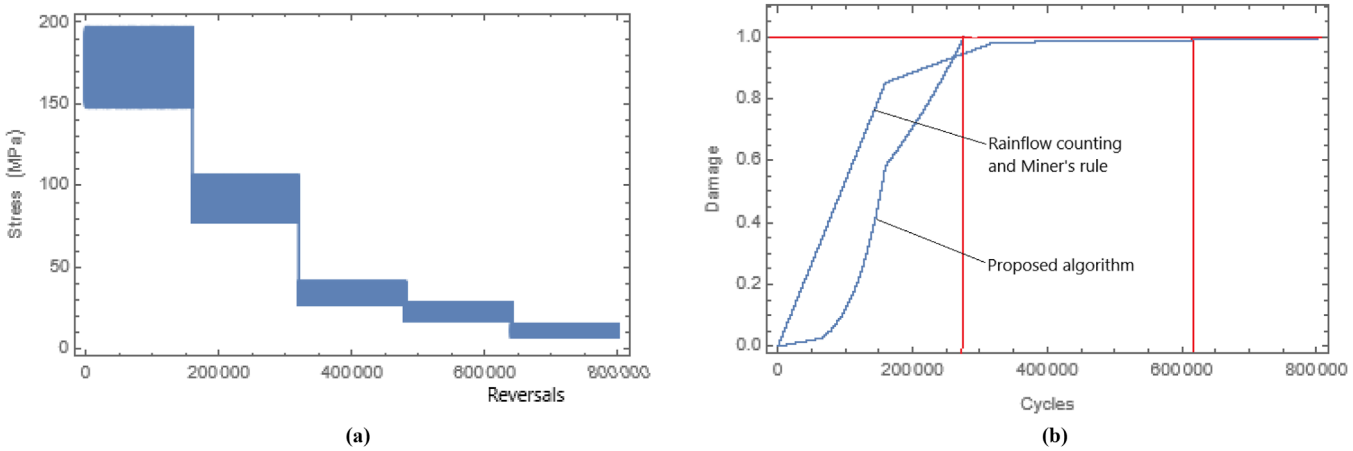

FIGURE 17 (a) Decreasing amplitude multi-stage random loading, (b) damage accumulation simulation and fatigue life prediction with the aid of the proposed and the existing method

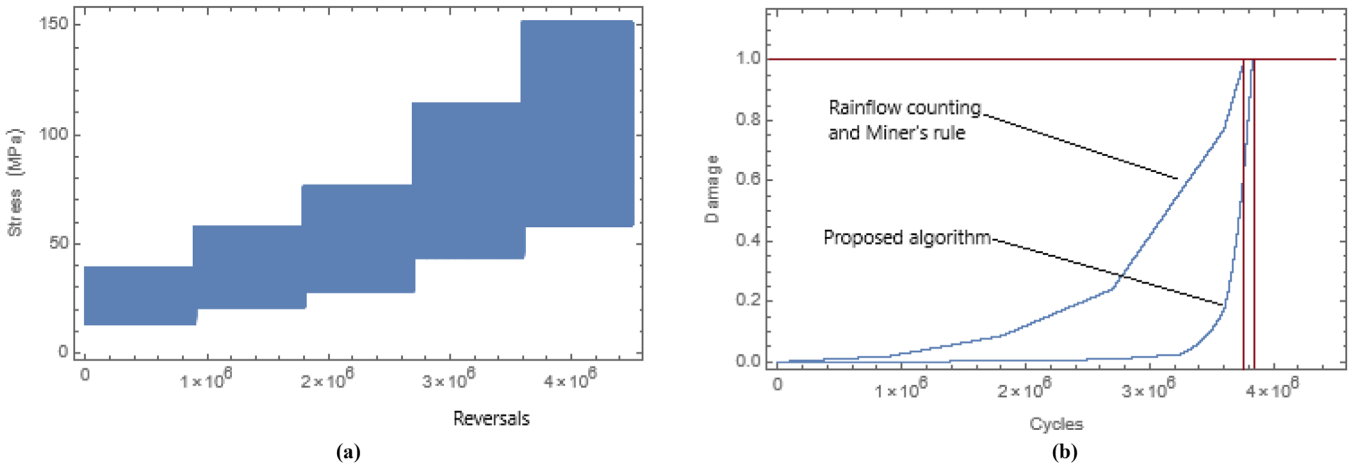

FIGURE 18 (a) Increasing amplitude multi-stage random loading, (b) damage accumulation simulation and fatigue life prediction with the aid of the proposed and the existing method

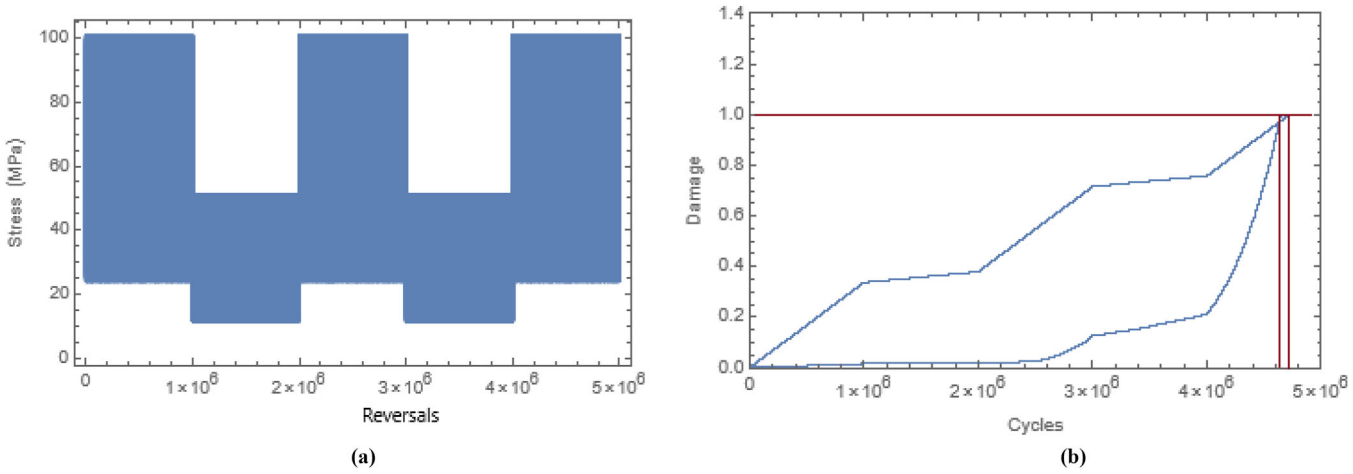

FIGURE 19 (a) Alternating block amplitude multi-stage random loading, (b) damage accumulation simulation and fatigue life prediction with the aid of the proposed and the existing method

TABLE 1 Loading spectra and comments on the obtained results

Loading type	Range of randomstress values (MPa)	Deviation of the predicted fatigue life with respect to the existing method	Comments
One-stage random loading	0–500	−2.23%	Good agreement between the results of the proposed and the existing method. The existing method overestimates slightly the fatigue life
High-low two-stage random loading	First block: 10–100 Second block: 10–55	−18.77%	Quite large deviation between the results of the proposed and the existing method. The existing method overestimates considerably the fatigue life
Low-high two-stage random loading	First block: 10–60 Second block: 10–110	1.43%	Good agreement between the results of the proposed and the existing method. The existing method underestimates slightly the fatigue life
Multi-stage spectrum with decreasing random stress range	First block: 150–195 Second block: 80–104 Third block: 30–39 Fourth block: 20–26 Fifth block: 10–13	−59.16%	Quite large deviation between the results of the proposed and the existing method. The existing method overestimates considerably the fatigue life
Multi-stage spectrum with increasing random stress range	First block: 15.0–37.5 Second block: 22.5–56.25 Third block: 30.0–75.0 Fourth block: 45.0–112.5 Fifth block: 60.0–150.0	2.18%	Good agreement between the results of the proposed and the existing method. The existing method underestimates slightly the fatigue life
Multi-stage spectrum with alternating random stress range	First block: 25.0–100.0 Second block: 12.5–50.00 Third block: 25.0–100.0 Fourth block: 12.5–50.0 Fifth block: 25.0–100.0	−1.53%	Good agreement between the results of the proposed and the existing method. The existing method overestimates slightly the fatigue life

TABLE 2 Processing time and fatigue life prediction for combinations of the proposed tools with the rainflow counting method and Miner's linear damage rule

Counting method	Damage accumulation model	Loading spectrum	Processing time	Predicted fatigue life (cycles)
Rainflow method	Miner's rule	One-stage random loading	13.845 h	30,412
		High-low two-stage random loading	53.610 h	5,898,138
		Low-high two-stage random loading	50.532 h	5,181,081
		Multi-stage spectrum with decreasing random stress range	3.911 h	622,642
		Multi-stage spectrum with increasing random stress range	32.228 h	3,761,711
		Multi-stage spectrum with alternating random stress range	43.017 h	4,711,222
Proposed counting method	Proposed damage accumulation model	One stage random loading	426 s	29,735
		High-low two-stage random loading	1939 s	4,791,344
		Low-high two-stage random loading	2053 s	5,255,528
		Multi-stage spectrum with decreasing random stress range	134 s	254,186
		Multi-stage spectrum with increasing random stress range	1341 s	3,843,340
		Multi-stage spectrum with alternating random stress range	1761 s	4,639,711
Rainflow method	Proposed damage accumulation model	One stage random loading	14.404 h	29,629
		High-low two-stage random loading	54.991 h	4,791,188
		Low-high two-stage random loading	53.081 h	5,255,410
		Multi-stage spectrum with decreasing random stress range	4.087 h	254,171
		Multi-stage spectrum with increasing random stress range	34.333 h	3,843,192
		Multi-stage spectrum with alternating random stress range	46.427 h	4,639,582
Proposed counting method	Miner's rule	One-stage random loading	498 s	31,222
		High-low two-stage random loading	2299 s	4,918,511
		Low-high two-stage random loading	2490 s	5,008,198
		Multi-stage spectrum with decreasing random stress range	153 s	282,107
		Multi-stage spectrum with increasing random stress range	1537 s	3,518,918
		Multi-stage spectrum with alternating random stress range	2082 s	4,677,101

The comparison of the fatigue damage accumulation and life prediction results is demonstrated in Figure 19b. These findings indicate that the alternating stress range in a sequence high-low-high-low-high causes the cancellation of the overloading effects by the underloading ones and yields good agreement in the life predictions between the proposed nonlinear algorithm and the existing linear one. The description of the selected loading spectra and the main conclusions are summarized in Table 1. The impact on the processing time and the fatigue life prediction of several combinations of the proposed tools with the existing counting method and Miner's linear model are summarized in Table 2. Results for the combination of Miner's rule and rainflow method, proposed damage summation tool and proposed counting method, proposed damage summation rule and rainflow method, and Miner's rule and proposed counting method have been presented for the selected six loading cases: one-stage random loading, H/L two-stage loading, L/H two-stage loading, multistage spectrum with decreasing stress range, multistage spectrum with increasing stress range, multistage spectrum with alternating stress range. The computation was carried out with the software Wolfram Mathematica version 12.3 in a PC with processor Intel(R) Core(TM) i7-5600U CPU @ 2.60 GHz 2.59 GHz and installed RAM 8.00 GB. The processing time in seconds has been obtained with the aid of the command *AbsoluteTiming[expr]*.

5 | CONCLUSION

A new nonlinear algorithm for fatigue damage accumulation estimation and life prediction for structures under irregular loading spectra is proposed. The new algorithm has two modules: (a) a new cycle counting method, and (b) a new multilinear damage summation method. The results of the new algorithm are compared with the results of the existing rainflow counting method and Miner's linear damage summation rule that

is adopted by the design codes Eurocode, AISC, and DNV-GL.

Unlike the existing standard method, the proposed method is consistent with the nonlinear material mechanisms during fatigue and takes into account the loading sequence effects. Therefore, apart from realistic fatigue damage estimation and life prediction, it can be adopted for reliable real-time structural health monitoring. It is also suitable for developing inspection plans that are consistent with the aging mechanisms of the materials.

The proposed method has been implemented into six representative loading types: (a) uniform random loading, (b) high-low two-stage random loading, (c) low-high two-stage random loading, (d) multi-stage spectrum with decreasing random stress range, (e) multi-stage spectrum with increasing random stress range, and (f) multi-stage spectrum with alternating random stress range. The obtained results have indicated good agreement in life prediction between the proposed and the existing method only in spectrum loadings where the overloading effects are canceled by the underloading ones. Indeed, the deviation of the results in the spectrum loading type (a) and (f) was only 2.23% and 1.53%, respectively, with a trend the existing method to overestimate slightly the fatigue life. The implementation of the proposed method into two-stage low-high and multistage low-high loading spectra has also provided very good agreement between the proposed and the existing method with a trend the existing method to underestimate slightly the fatigue life. Unlike the later findings, the implementation of the proposed algorithm into two-stage high-low and multistage high-low loading spectra has resulted in large deviation between the proposed and the existing method. The deviation of the results in the spectrum loading type (b) and (d) has been 18.77% and 59.16%, respectively. These results have indicated that the existing method overestimates considerably the fatigue life and yields unsafe predictions to loading spectra of decreasing stress amplitude. All in all, the proposed algorithm has demonstrated its ability to predict the loading sequence effects and especially the fatigue life reduction of structures under loading spectra that cause overloading at the early stages of structures' life where the design codes yield unsafe life prediction. The novel elements of the proposed method are the new counting and nonlinear damage summation algorithms for spectrum loading histories. The proposed method has almost the same reliability as the rainflow method and much better numerical efficiency. The new multilinear damage summation algorithm provides for the first time the advantages of the nonlinear fatigue life prediction in spectrum loading and predicts the loading sequence effects. However, the method is limited to uniaxial fatigue. Expansion of the method to multiaxial fatigue is the next step.

REFERENCES

Adeli, H., & Alrijleh, M. M. (1987). A knowledge-based expert system for design of roof trusses. *Computer-Aided Civil and Infrastructure Engineering*, *2*(3), 179–195.

Adeli, H., & Balasubramanyam, K. V. (1988a). A knowledge-based system for design of bridge trusses. *Journal of Computing in Civil Engineering, ASCE*, *2*(1), 1–20.

Adeli, H., & Balasubramanyam, K. V. (1988b). A novel approach to expert systems for design of large structures. *AI Magazine 1988*(Winter), 54–63.

Adeli, H., & Hung, S. L. (1994). An adaptive conjugate gradient learning algorithm for effective training of multilayer neural networks. *Applied Mathematics and Computation*, *62*(1), 81–102.

Adeli, H., & Hung, S. L. (1995). *Machine learning–neural networks, genetic algorithms, and fuzzy systems*. John Wiley and Sons.

Adeli, H., & Paek, Y. (1986a). Computer-aided design of structures using LISP. *Computers and Structures*, *22*(6), 939–956.

Adeli, H., & Paek, Y. (1986b). Computer-aided analysis of structures in INTERLISP environment. *Computers and Structures*, *23*(3), 393–407.

Adeli, H., & Yeh, C. (1989). Perceptron learning in engineering design. *Computer-Aided Civil and Infrastructure Engineering*, *4*(4), 247–256.

Adeli, H., & Yeh, C. (1990). Explanation-based machine learning in engineering design. *Engineering Applications of Artificial Intelligence*, *3*(2), 127–137.

Aeran, A., Siriwardane, S. C., Mikkelsen, O., & Langen, I. (2017). A new nonlinear fatigue damage model based only on S-N curve parameters. *International Journal of Fatigue*, *103*, 327–341.

Ahmadlou, M., & Adeli, H. (2010). Enhanced probabilistic neural network with local decision circles: A robust classifier. *Integrated Computer-Aided Engineering*, *17*(3), 197–210.

Amezquita-Sanchez, J. P., & Adeli, H. (2015). Feature extraction and classification techniques for health monitoring of structures. *Scientia Iranica–Transaction A: Civil Engineering*, *22*(6), 1931–1940.

Amezquita-Sanchez, J. P., & H Adeli, H. (2016). Signal processing techniques for vibration-based health monitoring of structures. *Archives of Computational Methods in Engineering*, *23*(1), 1–15.

ASTM (2011). Standard practices for cycle counting in fatigue analysis. E1049-85.

Athanasiou, A., Ebrahimkhanlou, A., Zaborac, J., Hrynyk, T., & Salamone, T. (2020). A machine learning approach based on multifractal features for crack assessment of reinforced concrete shells. *Computer-Aided Civil and Infrastructure Engineering* , *35*, 565–578.

Carpinteri, A., Ronchei, C., Scorza, D., & Vantadori, S. (2015). Critical plane orientation influence on multiaxial high-cycle fatigue assessment. *Physical Mesomechanics*, *18*(4), 348–354.

Carpinteri, A., & Spagnoli, A. (2001). Multiaxial high-cycle fatigue criterion for hard metals. *International Journal of Fatigue*, *23*(2), 135–145.

Carpinteri, A., Spagnoli, A., & Vantadori, S. (2017). A review of multiaxial fatigue criteria for random variable amplitude loads. *Fatigue and Fracture of Engineering Materials and Structures*, *40*, 1007–1036.

Correia, J. A. F. O., Raposo, P., Muniz-Calvente, M., Blason, S., Lesiuk, G., De, J. A. M. P., Moreira, P. M. G. P., Calcada, R. A. B., & Canteli, A. F. (2017). A generalization of the fatigue Kohout-Věchet model for several fatigue damage parameters. *Engineering Fracture Mechanics*, *185*, 284–300.

Dantas, R., Correia, J., Lesiuk, G., Rozumek, D., Zhu, S. -P., de Jesus, A., Susmel, L., & Berto, F. (2021). Evaluation of multiaxial high-cycle fatigue criteria under proportional loading for S355 steel. *Engineering Failure Analysis*, *120*, 105037.

Deng, J., Lu, Y., & Lee, V. C. (2020). Concrete crack detection with handwriting script interferences using faster region-based convolutional neural network. *Computer-Aided Civil and Infrastructure Engineering*, *35*(4), 373–388.

DNV-GL. (2015). *Fatigue methodology of offshore ships, DNVGL-RP-C206*. https://rules.dnv.com/docs/pdf/DNV/RP/2015-07/DNVGL-RP-C206.pdf

Fatemi, A., & Socie, F. (1988). A critical plane approach to multiaxial fatigue damage including out-of-phase loading. *Fatigue and Fracture of Engineering Materials and Structures*, *1*(3), 149–165.

Fatemi, A., & Yang, L. (1998). Cumulative fatigue damage and life prediction theories: A survey of the state of the art for homogeneous materials. *International Journal of Fatigue*, *20*, 9–34.

Hampshire, T. A., & Adeli, H. (2000). Monitoring the behavior of steel structures using distributed optical fiber sensors. *Journal of Constructional Steel Research*, *53*(3), 267–281.

Hashin, Z., & Rotem, A. (1978). A cumulative damage theory of fatigue failure. *Materials Science and Engineering*, *34*, 147–160.

Hectors, K., & De Waele, W. (2021). Cumulative damage and life prediction models for high-cycle fatigue of metals: A review. *Metals*, *11*, 204.

Horas, C. S., Correia, J. A. F. O., De Jesus, A. M. P., Kripakaran, P., & Calcada, R. (2017). Application of the modal superposition technique combined with analytical elastoplastic approaches to assess the fatigue crack initiation on structural components. *Engineering Fracture Mechanics*, *185*, 271–283.

Hung, S. L., & Adeli, H. (1993). Parallel backpropagation learning algorithms on CRAY Y-MP8/864 supercomputer. *Neurocomputing*, *5*(6), 287–302.

Hung, S. L., & Adeli, H. (1994). A parallel genetic/neural network learning algorithm for MIMD shared memory machines. *IEEE Transactions on Neural Networks*, *5*(6), 900–909.

Jiang, S., & Zhang, J. (2020). Real-time crack assessment using deep neural networks with wall-climbing unmanned aerial system. *Computer-Aided Civil and Infrastructure Engineering*, *35*, 549–564

Jiang, X., & Adeli, H. (2007). Pseudospectra, MUSIC, and dynamic wavelet neural network for damage detection of highrise buildings. *International Journal for Numerical Methods in Engineering*, *71*(5), 606–629.

Lara-Benıtez, P., Carranza-Garcıa, M., Garcıa-Gutierrez, J., & Riquelme, J. C. (2020). Asynchronous dual-pipeline deep learning framework for online data stream classification. *Integrated Computer-Aided Engineering*, *27*(2), 101–119.

Leming, M., Gorriz, J. M., & Suckling, J. (2020). Ensemble deep learning on large, mixed-site fMRI datasets in autism and other tasks. *International Journal of Neural Systems*, *30*(7), 2050012.

Liu, J., Yang, X., Lau, S., Wang, X., Luo, S., Lee, C. S., & Ding, L. (2020). Automated pavement crack detection and segmentation based on two-step convolutional neural network. *Computer-Aided Civil and Infrastructure Engineering*, *35*(11), 1291–1305.

Liu, Q., Gao, Y., Li, Y., & Xue, Q. (2020). Fatigue life prediction based on a novel improved version of the Corten-Dolan model considering load interaction effect. *Engineering Structures*, *221*, 111036.

Liu, X., Liu, Z., Liang, Z., Zhu, S. P., Correia, J. A. F. O., & De Jesus, A. M. P. (2019). PSO-BP neural network-based strain prediction of wind turbine blades., *Materials*, *12*(121), 2889.

Macha, E., & Niesłony, A. (2012). Critical plane fatigue life models of materials and structures under multiaxial stationary random loading: The state-of-the-art in Opole Research Centre CESTI and directions of future activities. *International Journal of Fatigue*, *39*, 95–102.

Matsubara, G., & Hayashida, A. (2021). Fatigue life prediction for the AISI 4340 steel under multiaxial variable-amplitude loading with respect to the calculated rainflow damage based on the path length. *International Journal of Fatigue*, *147*, 106181.

Matsuishi, M., & Endo, T. (1968). Fatigue of metals subjected to varying stress-fatigue lives under random loading. *Kyushu District Meeting, JSEM*, Fukuoka, Japan (pp. 37–40).

Miner, M. A. (1945). Cumulative damage in fatigue. *Journal of Applied Mechanics*, *12*, A159–A164.

Oh, B. K., Kim, K. J., Kim, Y., Park, H. S., & Adeli, H. (2017). Evolutionary learning based sustainable strain sensing model for structural health monitoring of high-rise buildings. *Applied Soft Computing*, *58*, 576–585.

Paek, Y., & Adeli, H. (1988b). STEELEX: A coupled expert system for integrated design of steel structures. *Engineering Applications of Artificial Intelligence*, *1*(3), 170–180.

Paek, Y., & Adeli, H. (1988a). Representation of structural design knowledge in a symbolic language. *Journal of Computing in Civil Engineering, ASCE*, *2*(4), 346–364.

Papadopoulos, I. V. (1994). A new criterion of fatigue strength for out-of- phase bending and torsion of hard metals. *Fatigue*, *16*, 377–384.

Park, H. S., Lee, H. M., Adeli, H., & Lee, I. (2007). A new approach for health monitoring of structures: terrestrial laser scanning. *Computer-Aided Civil and Infrastructure Engineering*, *22*(1), 19–30.

Pavlou, D. (2002). A phenomenological fatigue damage accumulation rule based on hardness increasing, for the 2024-T42 aluminum. *Engineering Structures*, *24*, 1363–1368.

Pavlou, D. (2018). The theory of the S-N fatigue damage envelope: Generalization of linear, double-linear, and non-linear fatigue damage models. *International Journal of Fatigue*, *110*, 204–214.

Pham Q. H., Gagnon M., Antoni J., Tahan A., Monette C. (2021). Rainflow-counting matrix interpolation over different operating conditions for hydroelectric turbine fatigue assessment. *Renewable Energy*, *172*, 465–476.

Qarib, H., & Adeli, H.,(2014). Recent advances in health monitoring of civil structures. *Scientia Iranica–Transaction A: Civil Engineering*, *21*(6), 1733–1742.

Rafiei, M. H., & Adeli, H. (2017a). A new neural dynamic classification algorithm. *IEEE Transactions on Neural Networks and Learning Systems*, *28*(12), 3074–3083 https://doi.org/10.1109/TNNLS.2017.2682102

Rafiei, M. H., & Adeli, H. (2017b). A novel machine learning based algorithm to detect damage in highrise building structures. *The Structural Design of Tall and Special Buildings*, *26*, 18. https://doi.org/10.1002/tal.1400

Rafiei, M. H., & Adeli, H. (2017c). NEEWS: A novel earthquake early warning system using neural dynamic classification and neural dynamic optimization model. *Soil Dynamics and Earthquake Engineering*, *100*, 417–427.

Rafiei, M. H., & Adeli, H. (2018). A novel unsupervised deep learning model for global and local health condition assessment of structures. *Engineering Structures*, *156*(1), 598–607.

Rafiei, M. H., Khushefati, W. H., Demirboga, R., & Adeli, H. (2017a). Novel approach for concrete mixture design using neural dynamics model and the virtual lab concept. *ACI Materials Journal*, *114*(1), 117–127. https://doi.org/10.14359/51689485

Rafiei, M. H., Khushefati, W. H., Demirboga, R., & Adeli, H. (2017b). Supervised deep restricted Boltzmann machine for estimation of concrete compressive strength. *ACI Materials Journal*, *114*(2), 237–244.

Rege, K., & Pavlou, D. (2017). A one-parameter nonlinear fatigue damage accumulation model. *International Journal of Fatigue*, *98*, 234–246.

Richards, F. D., LaPointe, N. R., & Wetzel, R. M. (1974). A cycle counting algorithm for fatigue damage analysis. *SAE Transactions*, *83*(2),1187–1197.

Sharifimehr, S., & Fatemi, A. (2019). Fatigue analysis of ductile and brittle behaving steels under variable amplitude multiaxial loading. *Fatigue and Fracture of Engineering Materials and Structures*, *42*, 1722–1742.

Si-Jian, L., Wei, L., Da-Qing, T., & Jun-Bi, L. (2018). A new fatigue damage accumulation model considering loading history and loading sequence based on damage equivalence. *International Journal of Damage Mechanics*, *27*, 707–728.

Sørensen, R. A., Nielsen, M., & Karstoft, H. (2020). Routing in congested baggage handling systems using deep reinforcement learning. *Integrated Computer-Aided Engineering*, *27*(2), 139–152.

Stafford, P., & Bommer, J. (2009). Empirical equations for the prediction of the equivalent number of cycles of earthquake ground motion. *Soil Dynamics and Earthquake Engineering*, *29*, 1425–1436.

Stellmach, S., Braun, L. N., Wachter, M., Esderts, A., & Diekhaus, S. (2021). On load assumptions for self-propelled forage harvesters. *International Journal of Fatigue*, *147*, 106114.

Subramanyan, S. (1976). A cumulative damage rule based on the knee point of the SN curve. *Journal of Engineering Materials and Technology*, *98*, 316–321.

Theil, N. (2016). Fatigue life prediction method for the practical engineering use taking in account the effect of the overload blocks. *International Journal of Fatigue*, *90*, 23–35.

Wang, M., & Cheng, J. C. P. (2020). A unified convolutional neural network integrated with conditional random field for pipe defect segmentation. *Computer-Aided Civil and Infrastructure Engineering*, *35*(2), 162–177.

Wang, N., Zhao, X., Zou, Z., Zhao, P., & Qi, F. (2020). Autonomous damage segmentation and measurement of glazed tiles in historic buildings via deep learning. *Computer-Aided Civil and Infrastructure Engineering*, *35*(3), 277–291.

Weingardt, R. G. (2010). Engineering legends—Hojjat Adeli. *Leadership and Management in Engineering*, *10*(2), 88–93. https://doi.org/10.1061/(ASCE)LM.1943-5630.0000059.

Xie, H., Liu, H., Tian, J., Shao, X., & Zhang, Y. (2021). Development and simple validation of the FAC_NPIC computer code for fatigue assessment. *International Journal of Pressure Vessels and Piping*, *191*, 104331.

Yu, S., & Zhang, J. (2020). Fast Bridge deflection monitoring through an improved feature tracing algorithm. *Computer-Aided Civil and Infrastructure Engineering*, *35*(3), 292–302.

Yue, J., Yang, K.e., Peng, L., & Guo, Y. (2021). A frequency-time domain method for ship fatigue damage assessment. *Ocean Engineering*, *220*, 108154.

Zhang, J., & Aoki, T. (2020). A frequency-domain noniterative algorithm for structural parameter identification of shear buildings subjected to frequent earthquakes. *Computer-Aided Civil and Infrastructure Engineering*, *35*, 615–627.

Zhu, S. P., Hao, Y. Z., Correia, J. A., Lesiuk, G., & de Jesus, A. M. (2019). Nonlinear fatigue damage accumulation and life prediction of metals: A comparative study. *Fatigue and Fracture of Engineering Materials and Structures*, *42*, 1271–1282.

Zhu, S. P., Liao, D., Liu, Q., Correia, J. A. F. O., & De, J. A. M. P. (2019). Nonlinear fatigue damage accumulation: Isodamage curve-based model and life prediction aspects., *International Journal of Fatigue*, *128*, 105185.

Zhu, S. P., Yu, Z. Y., Correia, J., & De Jesus, A. (2018). Evaluation and comparison of critical plane criteria for multiaxial fatigue analysis of ductile and brittle materials. *International Journal of Fatigue*, *112*, 279–288,

How to cite this article: Pavlou, D. A deterministic algorithm for nonlinear, fatigue-based structural health monitoring. *Comput Aided Civ Inf*. 2021;1–23. https://doi.org/10.1111/mice.12783

APPENDIX: PSEUDOCODE OF THE PROPOSED METHOD

*** Data

*** **sigmaR** is the matrix of random peaks and valleys before filtering

*** **sigmaA** is the matrix of random peaks and valleys after knee point and plateau removal

*** **Se** is the fatigue endurance limit of the material

*** **Su** is the ultimate stress of the material

*** **Ni** is the number of cycles up to failure according to the SN curve

*** **ns** is the number of random stress values

*** **nc** is the number of counted stress cycles

*** Generation of random values for sigma (with the aid of Wolfram Mathematica symbolic programming)

SigmaR[i] = Random number with certain minimum and maximum values

*** Knee point removal and plateau removal (with the aid of Wolfram Mathematica symbolic programming)

ABB : = Table[If[(sigmaR[[i + 2]] - sigmaR[[i + 1]])*(sigmaR[[i + 1]] - sigmaR[[i]]) > 0, sigmaR[[i + 1]] = sigmaR[[i]]], {i, 1, ns}];

sigmaA[i] = Delete Duplicates in ABB[i];

*** Counting algorithm

*** sigmaAP is a peak stress value before cycle counting

*** sigmaAV is a valley stress value before cycle counting

*** sigmaCP is the peak value of the counted stress cycle
*** sigmaCV is the valley value of the counted stress cycle
i = 0
For i = 0 to ns
i = i+1
If sigmaA[i] > sigmaA[i+1] then sigmaAP[i] = sigmaA[i] else sigmaAV[i] = sigmaA[i]
sigmaCP[i] = sigmaAP[i]
If (sigmaAP[i+1]- sigmaAV[i]) > (sigmaAP[i-1]- sigmaAV[i]) then
(sigmaCV[i-1] = sigmaAV[i] and sigmaCV[i+1] = 0) else
(sigmaCV[i-1] = 0 and sigmaCV[i+1] = sigmaAV[i])
Next i
*** Equivalent stress amplitude according to Goodman's Rule
*** sigmaCMEAN is the mean stress of a loading cycle
*** sigmaCAMP is the amplitude of a loading cycle
*** sigmaCEQ is the equivalent stress amplitude of a loading cycle
sigmaCMEAN[i] = (sigmaCP[i]+sigmaCV[i])/2
sigmaCAMP[i] = (sigmaCP[i]-sigmaCV[i])/2
sigmaCEQ[i] = sigmaCAMP[i]*(1- sigmaCMEAN[i]/ Su)^-1
*** Removal of loading cycles with equivalent amplitude less than the fatigue endurance limit Se
For i = 0 to ns
If sigmaCEQ[i] < Su then sigmaCEQ[i] = 0
Next i
*** Number of cycles up to failure according to the SN Curve
*** Nf is the number of cycles up to failure according to Basquin's rule for SN curve simulation
*** b and C are the coefficients of Basquin's rule
sigmaCEQ[i]*Nf[i]^b = C
For i = 0 to ns
Nf[i] = 10^(Log(C/ sigmaCEQ[i])/b)
Next i
*** Nonlinear damage summation
*** nb is the number of damage bands
*** j is the band index
*** i is the stress cycle index
*** D is the calculated damage 0 < D < 1
*** q is the exponent of the continuous nonlinear damage rule
D = (n/Nf)^q
D[0] = 0
For i = 1 to nc
If D[i–1] < 1/nb then j = 1 else
If 1/nb < D[i–1] < 2*(1/nb) then j = 2 else
If 2*(1/nb) < D[i–1] < 3*(1/nb) then j = 3 else
⋮If (nb–1)*(1/nb) < D[i–1] < nb*(1/nb) then j = nb else
Print i; Print "FAILURE"
q[i] = (sigmaCEQ[i]/Su)^–0.75
w[i,j] = (D[j] – D[j–1])/ (D[j]^(1/ q[i]) – D[j–1]^(1/ q[i]))
ΔD[i] = w[i,j]*(1/ Nf[i])
D[i] = D[i–1]+ ΔD[i]
Next i